STIFFNESS PROPERTIES OF FOAM-FILLED FABRIC STRUCTURES

by Jerry W. Deaton and George W. Zender

Langley Research Center

Langley Station, Hampton, Va.
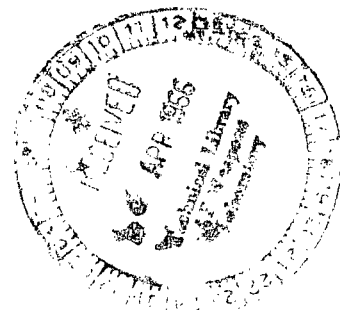
STIFFNESS PROPERTIES OF FOAM-FILLED FABRIC STRUCTURES

By Jerry W. Deaton and George W. Zender

Langley Research Center
Langley Station, Hampton, Va.

NATIONAL AERONAUTICS AND SPACE ADMINISTRATION

STIFFNESS PROPERTIES OF FOAM-FILLED FABRIC STRUCTURES

By Jerry W. Deaton and George W. Zender
Langley Research Center

SUMMARY

Results on both foam-filled and air-inflated fabric structures subjected to uniaxial, biaxial, shear, or bending stresses are presented and discussed. The results indicate that the stiffness properties of the foam-filled models are superior to those of the air-inflated models when compared on a mass-stiffness basis. The results also indicate that the stiffness properties of the foam are not proportional to foam density (stiffness increases faster than density) for the range of foam density of the investigation. The highest values of stiffness for both the air-inflated and the foam-filled models are obtained when the greater yarn count of the fabric is oriented in the longitudinal direction of the specimen. The values of Poisson's ratio for the foam-filled beams were, in general, less than the values usually encountered for isotropic materials. The results also indicate that the strength in shear for the foam-filled cylinders varies linearly with foam density and increases at about the same rate as foam density.

INTRODUCTION

Expandable structures fabricated from films or fabric materials and utilizing gases or foams for expansion and rigidization in space are being considered for many aerospace applications. A particular fabric construction which has been used at the Langley Research Center in studies (see refs. 1 and 2) of inflatable structures is known as Airmat and was developed by the Goodyear Aerospace Corporation. These studies have utilized air for inflation. Contained herein are the results of an investigation to determine the material properties of a particular nylon-neoprene fabric (manufacturer's designation XA27A119) by using a rigid closed-cell polyurethane foam for expansion and rigidization. Results on air-inflated models are presented for comparison with the foam-filled models.

SYMBOLS

The units used for the physical quantities defined in this paper are given both in the U.S. Customary Units and in the International System of Units (SI). Conversion factors pertinent to the present investigation are presented in the appendix and in reference 3.

A	cross-sectional area, $inch^2$ $(meter^2)$
c	distance from neutral axis to outermost element, inches (meters)
d	diameter, inches (meters)
E	Young's modulus, pounds force/$inch^2$ (newtons/$meter^2$)
G	shear modulus, pounds force/$inch^2$ (newtons/$meter^2$)
I	moment of inertia, $inch^4$ $(meter^4)$
l	length, inches (meters)
M	bending moment, inch-pound force (meter-newtons)
m	mass per unit length, pounds mass/inch (kilograms/meter)
P	tensile or compressive load, pounds force (newtons)
P_i	longitudinal load per unit of circumference, pounds force/inch (newtons/meter)

$$R = \frac{E_2/E_1}{\rho_2/\rho_1}$$

T	applied torque, inch-pounds force (meter-newtons)
t	thickness, inches (meters)
w	width, inches (meters)
γ	shear strain
ϵ	longitudinal or transverse strain
θ	angle of twist, degrees
μ	Poisson's ratio
ρ	density of foam, pounds mass/$foot^3$ (kilograms/$meter^3$)
τ	modulus of rupture, pounds force/$inch^2$ (newtons/$meter^2$)

Subscripts:

a   Airmat

f   foam

1,2   first or second value

TEST SPECIMENS AND METHOD OF TESTING

The fabric used for the present investigation consists of two surfaces tied together with "drop" yarns that provide a 1-inch (2.5-cm) space between surfaces when inflated. (See fig. 1.) Each surface consists of a nylon inner ply of Airmat weave with a coating of neoprene and a light nylon cover ply of plain weave which is also coated with neoprene. Other details of the fabric are given in table I and reference 1. Both the inner and cover ply shown in figure 1 contain one set of yarns (warp) with considerable crimp and another set of yarns (fill) which is more nearly straight. The inner and cover plies are oriented at 90° to each other so that the crimped yarns of one ply are alined with the more nearly straight yarns of the other ply. For purposes of specifying orientation of the fabric, the direction of the yarns of the heavier inner ply are employed; that is, the direction of the warp yarns of the inner ply is termed the warp direction of the fabric, whereas the direction tranverse to the warp direction is termed the fill direction. One set of specimens was made with the warp yarns and one set was made with the fill yarns oriented in the longitudinal direction of the specimens; hereinafter, the specimens with the warp yarns oriented in the longitudinal direction are referred to as warp specimens and the specimens with the fill yarns oriented in the longitudinal direction are referred to as fill specimens.

Three types of specimens were tested: a plain strip of the fabric, a cylinder, and a beam. General details of each type are shown in figure 2.

The strip specimens were clamped with aluminum plates at each end as indicated in figure 2(a) and were subjected to tensile loads with deadweights. The inner sides of the fabric were in contact during the tests rather than separated with extended drop yarns as indicated in figure 2(a).

Two types of cylinders were tested: One was air inflated and the other was filled with a rigid closed-cell polyurethane foam. The cylinders were made of one surface of the fabric obtained by severing the drop yarns between the two surfaces so that approximately 0.5 inch (1.3 cm) of the drop yarns remained with each surface. The surface was then fabricated into cylindrical form by splicing. The foam-filled cylinders employed

3

one splice as shown in figure 2(c), whereas the air-inflated cylinders utilized two diametrically opposite splices as shown in figure 2(d). Two air-inflated cylinder specimens were tested; one was a warp specimen and one was a fill specimen. Six foam-filled cylinders, two each of three nominal foam densities, were tested. (See table II.) One specimen of each foam density was a warp specimen and one of each foam density was a fill specimen.

The cylinder specimens were subjected to torsion and to longitudinal tensile loads as shown in figures 3 and 4. The foam-filled cylinders were also tested in compression by using a hydraulic testing machine with a capacity of 120 kips (534 KN). After all strain data were obtained on the foam-filled cylinder specimens, the specimens were tested to failure in torsion by using a torsion testing machine with a capacity of 60 000 inch-pounds (6780 m-N), as shown in figure 5.

Six foam-filled beam specimens (see fig. 2(b)), two each of three nominal foam densities (see table II), were tested. One specimen of each foam density was a warp specimen and one of each foam density was a fill specimen. The beam specimens were subjected to end bending moments as shown in figure 6. Two bending tests were made on each of the six beam specimens. One test was made with one side of the beam resting on the supporting fixture shown in figure 6 and the other test was made with the opposite side of the beam resting on the supports. For all bending tests the specimens were centered on the supports which were 10 inches (25.4 cm) apart. Bending moments were introduced by applying deadweight loads 7.5 inches (19.1 cm) from each support as shown in figure 6.

Strains on all specimens were measured with Tuckerman optical strain gages of 1- or 2-inch (2.5- or 5.1-cm) gage length. Longitudinal strains were obtained at the midlength of each specimen and transverse strains were also obtained at the midlength of each surface of the foam-filled beam specimens. In addition, shear strains were also measured on the foam-filled cylinder specimens. One of the characteristics of woven materials is that the strain under load is time dependent (see ref. 1) and careful timing is required to obtain useful strain data from specimens. For all specimens, loads were applied without unloading until maximum load was reached and the strain measurements were obtained at each load increment after sufficient time had elapsed (approximately 5 minutes) for the strain to be essentially constant with time.

The twist at the loaded end of the air-inflated and foam-filled cylinder specimens was measured by using an indicating arm attached to the wooden end piece and a protractor of 15-inch (38.1-cm) radius mounted to the supporting frame shown in figure 3. For the torsion failure testing of the foam-filled cylinder specimens, relative twist measurements were obtained from two indicating arms attached to the cylinder 10 inches (25.4 cm) apart and from two protractors of 14-inch (35.6-cm) radius. (See fig. 5.) Twist

4

measurements were obtained by using the same loading and time procedure as previously described. Internal pressure of the air-inflated cylinders was measured with a Bourdon tube pressure gage with a range of 0 to 15 psig (0 to 103.4 kN/m^2). All tests were performed at room temperature (approximately 75° F (300°K)).

After all tests were completed, foam density measurements were made on samples taken from each of the foam-filled specimens. Five foam samples were taken along the length of each cylinder and values of foam density were obtained. The results are shown in figure 7. It is evident from the figure that a definite density variation occurs along the length of the cylinder specimens. The variation of foam density with cylinder length, along with the shape and orientation of small foam cells observed in the samples, indicates that the cylinders were probably foamed with the longitudinal direction of the cylinder in a vertical position. Density measurements were made on three samples taken from each beam specimen along its length. These measurements did not indicate a variation in density with length of specimen as was obtained with the cylinder specimens. Table II gives the average of foam densities obtained from the samples taken from each specimen.

RESULTS

Strips and Air-Inflated Cylinders

Figure 8 shows a typical set of stress-strain results for the strip specimens and the air-inflated cylinder specimens. The symbols show the average of the strains measured on opposite sides of the specimens. The data shown by the curve faired through the circular symbols are for the strip specimens subjected to uniaxial loading. The lighter solid curve labeled "due to pressure" shows the longitudinal strain obtained for values of the longitudinal load per unit of circumference P_i for the cylinder as the pressure was slowly increased to 15.0 psig (103.4 kN/m^2), and the dashed curve indicates the longitudinal strains for decreasing pressures. Also shown in figure 8 are the longitudinal strains obtained for longitudinal tensile loads that were applied after the cylinder was in an initial state of tension due to internal pressure. Longitudinal strains were obtained as the internal pressure was slowly increased until the desired pressure level was obtained. Then the pressure was held constant and longitudinal tensile loads were introduced. Tensile loads were applied at pressure levels of 2.5 to 15.0 psig (17.2 to to 103.4 kN/m^2) in increments of 2.5 psig. Only data for pressures of 2.5, 7.5, and 15.0 psig (17.2, 51.7, and 103.4 kN/m^2) are shown in figure 8. The values of longitudinal stiffness Et shown in figure 8 were obtained from the slopes of the nearly linear curves faired through the data points. For the warp cylinder the stiffness values for the six pressure levels varied from 926 to 976 lbf/in. (162.2 to 170.9 kN/m) and had an average

value of 957 lbf/in. (167.6 kN/m). The longitudinal stiffnesses for the fill cylinder varied from 719 to 776 lbf/in. (125.9 to 135.9 kN/m) and had an average value of 754 lbf/in. (132.0 kN/m) for the six pressure levels. The longitudinal stiffnesses obtained for the warp and fill strip specimens were 739 lbf/in. (129.4 kN/m) and 471 lbf/in. (82.5 kN/m), respectively. The difference in stiffness values for the pressurized cylinders and strip specimens is to be expected since the two specimens are under different stress conditions. (See ref. 1.)

Figure 9 shows the torque-twist results obtained with the air-inflated cylinders for values of the longitudinal pressure stress P_i (various pressure levels). For small values of torque or twist, the shear stiffness Gt (based on elementary torsion theory with the effect of the splices neglected) is about 65 lbf/in. (11.4 kN/m) for both the fill and the warp cylinders at all the pressure stresses. The shear stiffness decreases as the torque or twist increases, and it becomes dependent on the pressure stress. No visible wrinkling or buckling of the cylinders was observed for the range of loads included in figure 9.

Foam-Filled Cylinders Subjected to Tension, Compression, and Torsion

Figure 10 shows a typical set of results for the foam-filled cylinder specimens subjected to longitudinal tensile and longitudinal compressive loads. The symbols show the average strains measured on opposite sides of the specimens. The data shown are for cylinders having a foam density of 2.0 lbm/ft^3 (32.0 kg/m^3). The circular symbols indicate the strains measured as tensile loads were applied to the cylinder (see fig. 4) and the square symbols indicate the measured strains for the specimens under applied compressive loads. Also indicated in figure 10 by the dashed lines are the load-strain curves corresponding to the average value of longitudinal stiffness for the pressurized cylinders under direct tensile load. The curves labeled "foam" in figure 10 represent the load-strain characteristics for the foam alone, based on the assumption that the fabric has the same value of stiffness in tension and compression and the same value as the average given previously. These curves were obtained by selecting a value of strain and then subtracting the corresponding load of the dashed curve from the load (for the same value of strain) of the curve faired through the data points. Data similar to those shown in figure 10 were obtained for each of the foam-filled cylinder specimens. The slope of the curves labeled "Foam" in figure 10 was used to obtain the tensile modulus and compressive modulus of the foam for the cylinder specimens. The values of tensile and compressive moduli were obtained by dividing the slope value of the curves labeled "foam" in figure 10 by the average cross-sectional area of the foam inside the cylinder specimen. The average cross-sectional area was obtained from the average of 10 diameter measurements made along the length of each foam-filled cylinder specimen; the average of the 10 diameter measurements is listed in table II. A value of 0.024 in. (0.061 cm) was used

for a single thickness of the fabric in the computations for determining the cross-sectional area.

Figure 11 shows the tensile modulus and compressive modulus of the foam plotted against foam density for the cylinder specimens. Solid lines have been faired through the data and extended by the dashed lines to the intersection of the ordinate and abscissa axes since zero modulus would be expected for zero density. For comparison, the broken curve shown in figure 11 indicates the modulus increasing at the same rate as the foam density, or $R = 1$, where R is defined by $R = \dfrac{E_2/E_1}{\rho_2/\rho_1}$. Thus, values of R greater than 1 indicate the modulus increasing faster than the density and values of R less than 1 indicate the density increasing faster than the modulus.

Figure 12 shows a typical set of results for the foam-filled cylinder specimens subjected to small torsion loads. (See fig. 3.) The symbols show the average shear strains measured on opposite sides of the specimens. The data shown are for cylinder specimens having a foam density of 3.8 lbm/ft^3 (60.9 kg/m^3). Also indicated in figure 12 by the dashed lines are the torque—shear-strain curves corresponding to a shear stiffness of 65 lbf/in. (11.4 kN/m) obtained from figure 9 for the pressurized cylinder specimens. The curves labeled "foam" in figure 12 represent the torque—shear-strain characteristics of the foam and were obtained by using the method previously described for determining the tensile and compressive moduli of the foam. Data similar to those shown in figure 12 were obtained for each of the cylinder specimens and elementary torsion theory was used to determine the shear modulus of the foam from the slope of the curves labeled "foam" in figure 12. Figure 13 shows the shear modulus of the foam plotted against foam density. The curve for $R = 1$ is also shown in figure 13 and is indicated by the broken line.

An index of the ultimate strength in torsion of the foam-filled cylinder specimens was obtained by twisting the specimens to failure and noting the value of ultimate torque. The values of ultimate torque were used to compute the modulus of rupture τ and the results are shown in figure 14 plotted against foam density. A value of the rupture modulus for the warp specimen having a foam density of 3.8 lbm/ft^3 (60.9 kg/m^3) was not obtained because failure for this specimen occurred in the bonded joint between the cylinder and the wooden end piece used to apply torque to the cylinder. Also indicated on the figure by the broken curve is $R = 1$.

A comparison of the specific stiffness EA/m between the foam-filled and air-inflated cylinder specimens is shown in figure 15. The data shown are for the cylinder specimens under longitudinal tensile loads. (See fig. 4.) The values of EA for the air-inflated cylinders were obtained from the curves of figure 8, whereas the values of EA for the foam-filled cylinders were obtained from curves similar to those shown in

figure 10. The value of m was taken as the mass per unit length for each specimen and included the mass of the inflation medium.

Beams Subjected to Bending Moment

Table III shows the sectional properties of the foam-filled beam specimens used to determine the mechanical properties of the beams. The sectional properties were evaluated from the assumed cross section which closely approximated the actual cross section as indicated by the sketch accompanying the table. For the calculations, the effective thickness of the fabric in the splice region was taken as 1.24 times that of the remainder of the beam for the beam with the warp yarns in the longitudinal direction, whereas the similar value for the beam with the fill yarns in the longitudinal direction was 1.46. These values were taken from reference 1 for beams of similar construction and represent the increase in stiffness of the spliced region over the stiffness of the remainder of the beam as determined from uniaxial tests.

Figure 16 shows a typical set of results for the foam-filled beam specimens. The data shown are for the warp beam with a foam density of 4.5 lbm/ft^3 (72.1 kg/m^3) and for the fill beam with a foam density of 4.9 lbm/ft^3 (78.5 kg/m^3). The solid curves faired through the data points are for increasing bending moment and the dashed curves are for decreasing bending moment. Also shown in figure 16 are the values of Poisson's ratio, obtained from the ratio of the transverse strain to the longitudinal strain at the various bending-moment levels, for increasing moment and for decreasing moment. Data similar to those shown in figure 16 were obtained for each of the six beam specimens and stiffnesses for the specimens were obtained from the slopes of the curves faired through the data for the longitudinal strains of the tension and compression sides of the beams. From these data the modulus of the foam was determined by using elementary bending theory, given by the equation

$$E_f = \frac{\dfrac{Mc}{\epsilon} - Et_a \dfrac{I_a}{t_a}}{I_f} \tag{1}$$

for beams of two materials having centroids lying in the same plane. The values of M/ϵ were taken as the average of the slopes of the curves faired through the data for the longitudinal strains measured on the tension and compression sides of the beams. (See fig. 16.) The value of Et_a was taken as the average value of the longitudinal stiffnesses for the pressurized cylinders under direct tensile load. (See fig. 8.) Values for the effective moment of inertia divided by the unspliced thickness I_a/t_a of the fabric and for the moment of inertia I_f of the foam were taken for the beam with the assumed cross section and listed in table III.

8

Values of the foam modulus E_f for the beam specimens in bending are shown in figure 17. The data shown in figure 17 are the average values of the foam modulus obtained from the two bending tests made on each beam as previously mentioned. The broken curve shown in figure 17 indicates that $R = 1$.

Figure 18 shows the effect of foam density on Poisson's ratio. It is evident from figure 16 that the average of values of Poisson's ratio for loading and unloading varies somewhat with bending moment up to a value of about 15 in-lbf (1.7 m-N); then the average of values remains approximately constant for increasing and decreasing bending moments for the range of bending moment above 15 in-lbf included in the investigation. This behavior in Poisson's ratio was characteristic for all bending tests and for this reason the values of Poisson's ratio shown in figure 18 are the average values for increasing and decreasing bending moments above 15 in-lbf of applied moment.

Figure 19 gives a specific-stiffness EI/m comparison between the foam-filled beams of the present investigation and the pressurized beams of reference 1. The values of EI for the foam-filled beams were taken as the average value from the two bending tests previously described and were obtained from curves similar to those shown in figure 16. For the pressurized beams the values of EI were obtained by taking the product of the average values of stiffness and the effective moment of inertia of the beams. (See fig. 9 and table II, respectively, of ref. 1.) The value of m was again taken as the mass per unit length for each specimen and included the mass of the inflation medium.

DISCUSSION

It is evident from figure 8 that for the air-inflated cylinders the tension stiffness in the warp direction is considerably more than the tension stiffness in the fill direction. This difference is mainly due to the yarn count being higher in the warp direction than in the fill direction of the fabric. (See table I.) Comparison of the tension and compression data for the foam-filled specimens (see figs. 10 and 16) indicates that the compression stiffness is approximately the same as the tension stiffness. This can be attributed to the overriding effect of the foam. Since the foam is much stiffer than the fabric (see figs. 10 and 16) and the ratio of foam area to fabric area is large, then, any compressive loads would be carried mostly by the foam without regard to fabric orientation. Figures 10 and 16 also indicate that for the foam-filled specimens both the tension and compression stiffnesses in the warp direction are greater than the corresponding stiffnesses in the fill direction but the difference is not as great as that for the air-inflated specimens. For example, for the air-inflated cylinders the tension stiffness for the fill specimen is approximately 78 percent of that for the warp specimen, whereas for the foam-filled cylinders the tension stiffness for the fill specimen is approximately 88 percent of that for the warp

specimen. Thus, the difference in yarn count in the warp and fill directions of the fabric also influences the stiffness of the foam-filled specimens.

It is evident from figures 11 and 17 that increased foam density has a beneficial effect on the tensile and compressive moduli of the foam. This effect can be seen by a comparison of the curves faired through the data with the broken curves which represent the density increasing at the same rate as the modulus (or $R = 1$). Favorable values of R were obtained for the foam-filled specimens; in figures 11 and 17 the modulus increases by a factor of approximately 2.3 as the corresponding foam densities increase by a factor of only approximately 1.9.

The average values of Poisson's ratio shown in figure 18 are, in general, less than the values usually encountered for isotropic materials. The results show that the values of Poisson's ratio increase with increasing foam density. This increase is possibly caused by physical differences in the cell structure of the foam at the various densities. At the lower value of foam density the cell structure is such that the shape and size of the cells vary considerably, whereas the cell structure of the foam at the higher foam densities is more constant and therefore performs as a more homogeneous material.

The results shown in figure 13 indicate that favorable values of R are also obtained for the foam-filled cylinder specimens in shear. Comparison of figures 11 and 13 indicates that, for the range of foam density contained herein, the values of R obtained for the cylinder specimens are approximately the same, regardless of stress conditions present. Comparison of figures 11 and 13 also shows that the value of shear modulus is about three-tenths of the tensile modulus of the foam at corresponding foam densities. This factor demonstrates a lower shear modulus of the foam as compared with those of isotropic materials for which the shear modulus is usually about four-tenths of the tensile modulus.

The results shown in figure 14 indicate that the ultimate shear strength of the foam varies almost linearly with the foam density and increases at about the same rate as the density.

Figure 15 indicates that the specific stiffness for the foam-filled cylinder specimens varies from approximately 33 to 47 times the specific stiffness for the air-inflated specimens as the ratio of the mass per unit length of the foam-filled specimens to that of the air-inflated specimens varies approximately from 2.3 to 3.2. Therefore, from a specific-stiffness viewpoint the foam-filled cylinder specimens offer substantial tension-stiffness advantages over the air-inflated cylinders.

Figure 19 shows that the specific stiffness of the foam-filled beams is approximately 3.2 to 4.9 times the specific stiffness of the pressurized beams of reference 1. The ratio of the mass per unit length of the foam-filled beams to that of the pressurized

10

beams varies from 0.61 to 0.87. It should be noted that the larger mass of the pressurized beams is due to an extra heavy coating of neoprene (see ref. 1) and for this reason direct comparison with the foam-filled beams is not applicable. Even without the extra coating, the data indicate, however, that bending-stiffness advantages for the foam-filled beams are likely.

CONCLUDING REMARKS

The stiffness properties of a particular nylon-neoprene fabric subjected to uniaxial, biaxial, shear, or bending stresses as obtained from foam-filled models have been presented. These results were compared with results obtained from other models utilizing air for inflation. The results demonstrate that the stiffness of the foam-filled models was superior to the stiffness of the pressurized models when compared on a mass-stiffness basis. For example, the specific stiffness of the foam-filled cylinder specimens varied from approximately 33 to 47 times the specific stiffness of the air-inflated cylinders. The results also show that, for the range of foam density of the investigation, increased density has a beneficial effect on the modulus of the foam. The modulus for the foam-filled specimens increased by a factor of approximately 2.3 as the corresponding foam densities increased by a factor of only approximately 1.9. The values of Poisson's ratio for the foam-filled beams were, in general, less than the values usually encountered for isotropic materials. For the foam-filled cylinders, the strength in shear varied linearly with foam density and increased at about the same rate as foam density. The results also show that the highest values of stiffness are obtained, regardless of erection medium, when the direction of the greater yarn count of the fabric is oriented in the longitudinal direction of the specimen.

Langley Research Center,
National Aeronautics and Space Administration,
Langley Station, Hampton, Va., November 8, 1965.

APPENDIX

CONVERSION OF U.S. CUSTOMARY UNITS TO SI UNITS

The International System of Units (SI) was adopted by the Eleventh General Conference on Weights and Measures, Paris, October 1960, in Resolution No. 12 (ref. 3). Conversion factors for the units used herein are given in the following table:

Physical quantity	U.S. Customary Unit	Conversion factor (*)	SI unit
Density	lbm/ft^3	16.02	kilograms/meter^3 (kg/m^3)
Force	lbf	4.448	newtons (N)
Length	in.	0.0254	meters (m)
Specific stiffness:			
Beams, EI/m	in^3	1.607×10^{-4}	joules-meter^2/kilogram (J-m^2/kg)
Cylinders, EA/m . . .	in.	0.2491	joules/kilogram (J/kg)
Stress	psi = lbf/in^2	6.895×10^3	newtons/meter^2 (N/m^2)
Temperature	$^{o}F + 459.67$	5/9	degrees Kelvin (^{o}K)

*Multiply value given in U.S. Customary Unit by conversion factor to obtain equivalent value in SI Unit.

Prefixes to indicate multiples of units are as follows:

Prefix	Multiple
mega (M)	10^6
kilo (k)	10^3
centi (c)	10^{-2}

REFERENCES

1. Zender, George W.; and Deaton, Jerry W.: The Stiffness Properties of Stressed Fabrics as Obtained From Model Tests. NASA TN D-775, 1961.

2. Stroud, W. Jefferson: Experimental and Theoretical Deflections and Natural Frequencies of An Inflatable Fabric Plate. NASA TN D-931, 1961.

3. Mechtly, E. A.: The International System of Units — Physical Constants and Conversion Factors. NASA SP-7012, 1964.

TABLE I.- DETAILS OF FABRIC

Item	Inner ply	Cover ply
Yarn	Nylon	Nylon
Weave	Airmat	Plain
Warp count, yarns/in. (yarns/cm)	82 (32)	96 (38)
Fill count, yarns/in. (yarns/cm)	45 (18)	103 (41)
Drop-yarn count, yarns/in^2 (yarns/cm^2) . . .	116 (18)	

TABLE II.- DETAILS OF FOAM-FILLED SPECIMENS

(a) Beams

Yarn in longitudinal direction	ρ		Total mass		l		w		t	
	lbm/ft^3	kg/m^3	slugs	kg	in.	cm	in.	cm	in.	cm
Warp	3.3	52.9	0.0224	0.3269	26	66	6.34	16.10	1	2.5
Warp	3.8	60.9	.0242	.3532	26	66	6.34	16.10	1	2.5
Warp	4.5	72.1	.0273	.3984	26	66	6.34	16.10	1	2.5
Fill	2.9	46.5	.0221	.3225	26	66	6.34	16.10	1	2.5
Fill	3.7	59.3	.0245	.3576	26	66	6.34	16.10	1	2.5
Fill	4.9	78.5	.0275	.4013	26	66	6.34	16.10	1	2.5

(b) Cylinders

Yarn in longitudinal direction	ρ		Total mass		l		d	
	lbm/ft^3	kg/m^3	slugs	kg	in.	cm	in.	cm
Warp	2.0	32.0	0.0206	0.3006	18	46	4.13	10.49
Warp	2.8	44.9	.0243	.3546	18	46	4.14	10.52
Warp	3.8	60.9	.0297	.4334	18	46	4.12	10.46
Fill	2.0	32.0	.0210	.3065	18	46	4.08	10.36
Fill	2.8	44.9	.0248	.3619	18	46	4.13	10.49
Fill	3.8	60.9	.0294	.4291	18	46	4.11	10.44

TABLE III.- SECTIONAL PROPERTIES OF FOAM-FILLED BEAMS

0.5 in. (1.27 cm) 0.5 in. (1.27 cm)

5.3 in. (13.46 cm)

Enclosed area 6.09 in^2 (39.29 cm^2)

Outside to outside 1 in. (2.54 cm)

Trace of outer periphery of foam-filled beam   Assumed section
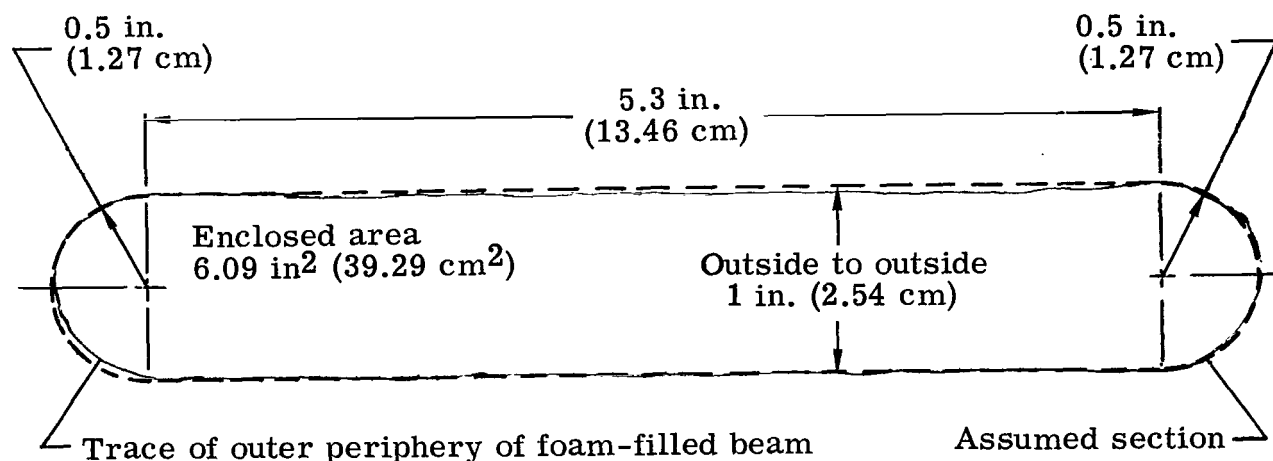
Property	Warp longitudinal		Fill longitudinal	
Fabric				
$\dfrac{\text{Effective thickness at splice}}{\text{Unspliced thickness}}$, K (see ref. 1)	1.24		1.46	
Effective periphery, in. (cm), for:				
Unspliced fabric, 2(5.3) in. or 2(13.46) cm	10.60	(26.92)	10.60	(26.92)
Spliced circle, $\pi(1)$K in. or $\pi(2.54)$K cm	3.89	(9.88)	4.58	(11.63)
Total	14.49	(36.80)	15.18	(38.55)
$\dfrac{\text{Effective moment of inertia}}{\text{Unspliced thickness}}$, $\dfrac{I_a}{t_a}$, in^3 (cm^3), for:				
Unspliced fabric, 2(5.3)(0.5)^2 in^3 or 2(13.46)(1.27)^2 cm^3 . . .	2.65	(43.42)	2.65	(43.42)
Spliced circle, $\pi(0.5)^3$K in^3 or $\pi(1.27)^3$K cm^3	.49	(8.03)	.57	(9.34)
Total	3.14	(51.45)	3.22	(52.76)
Foam				
Moment of inertia, I_f, in^4 (cm^4), for:				
Rectangular segment, $\dfrac{5.3(0.952)^3}{12}$ in^4 or $\dfrac{13.46(2.42)^3}{12}$ cm^4 . . .	0.381	(15.86)	0.381	(15.86)
Circular segments, $\dfrac{\pi(0.476)^4}{4}$ in^4 or $\dfrac{\pi(1.21)^4}{4}$ cm^4	.040	(1.66)	.040	(1.66)
Total	0.421	(17.52)	0.421	(17.52)
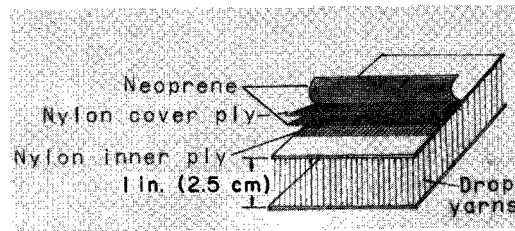
(a) Fabric.
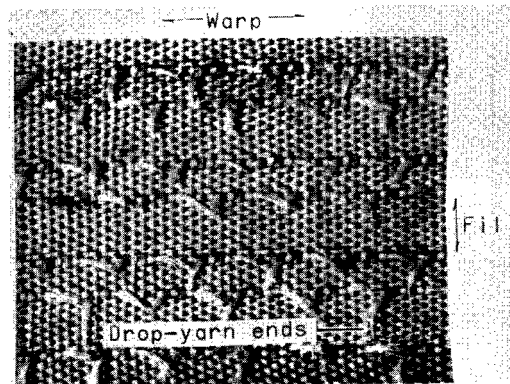
L-61-1072.1
(b) Photomicrograph of inner ply.

Figure 1.- Details of fabric construction.

16

3 in.
(7.6 cm)

1 in.
(2.5 cm)

Clamped by aluminum
end plates

8 in.
(20 cm)

12 in.
(30 cm)

(a) Strip.

5.3 in.
(13.5 cm)

6.3 in.
(16.0 cm)

26 in.
(66 cm)

(b) Beam.

Drop-yarn
ends

4 in.
(10 cm)

Width of two pieces
2 in. (5 cm) each

Width of piece for
splice 1 in. (2.5 cm)

18 in.
(46 cm)

(c) Foam-filled cylinder.

Splice width
.75 in.(1.91 cm)

4 in.
(10 cm)

Drop-yarn
ends

Splice width
.75 in. (1.91 cm)

15 in.
(38 cm)

18 in.
(46 cm)

Wood insert

(d) Air-inflated cylinder.
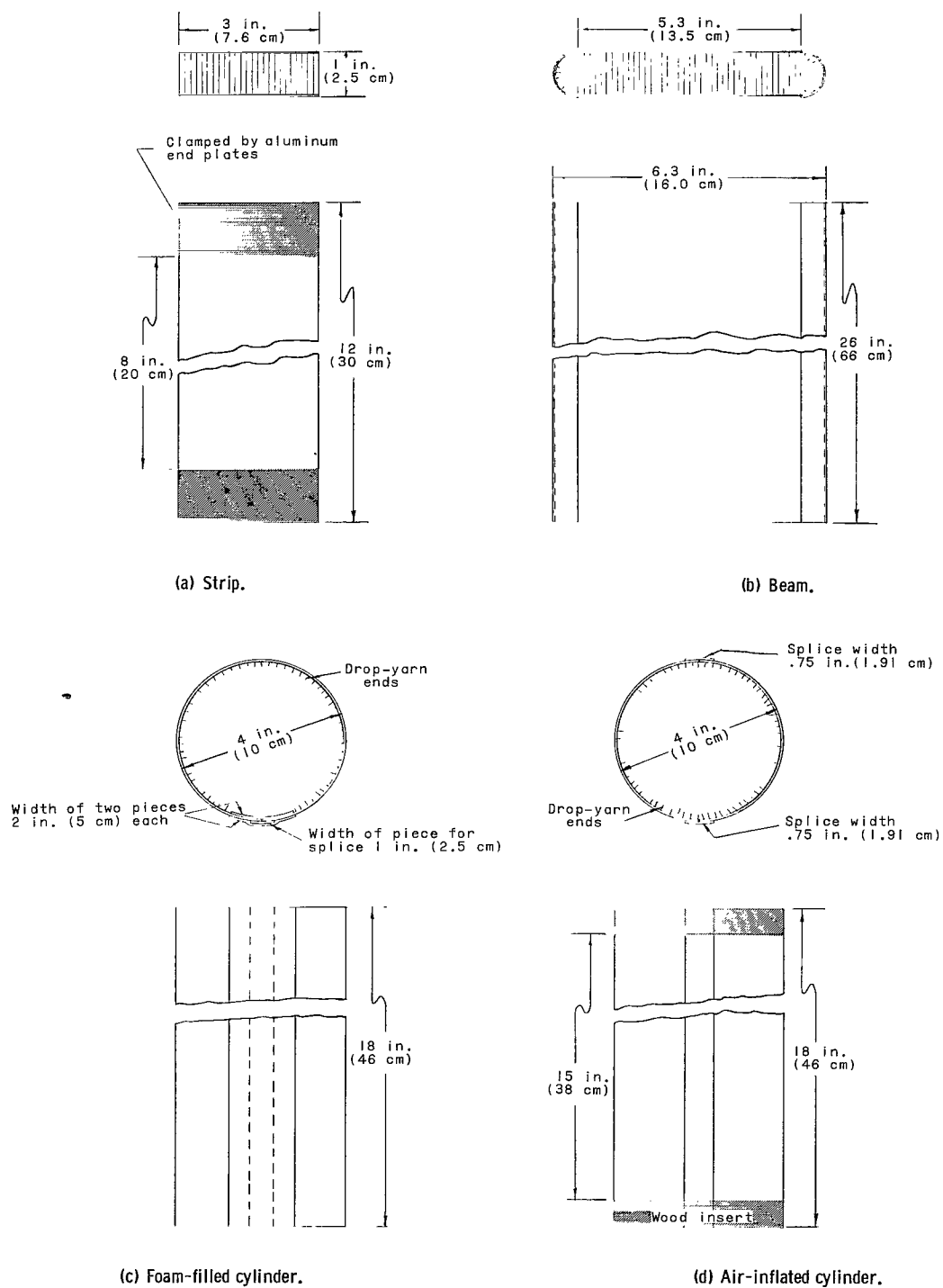
Figure 2.- Details of specimens.
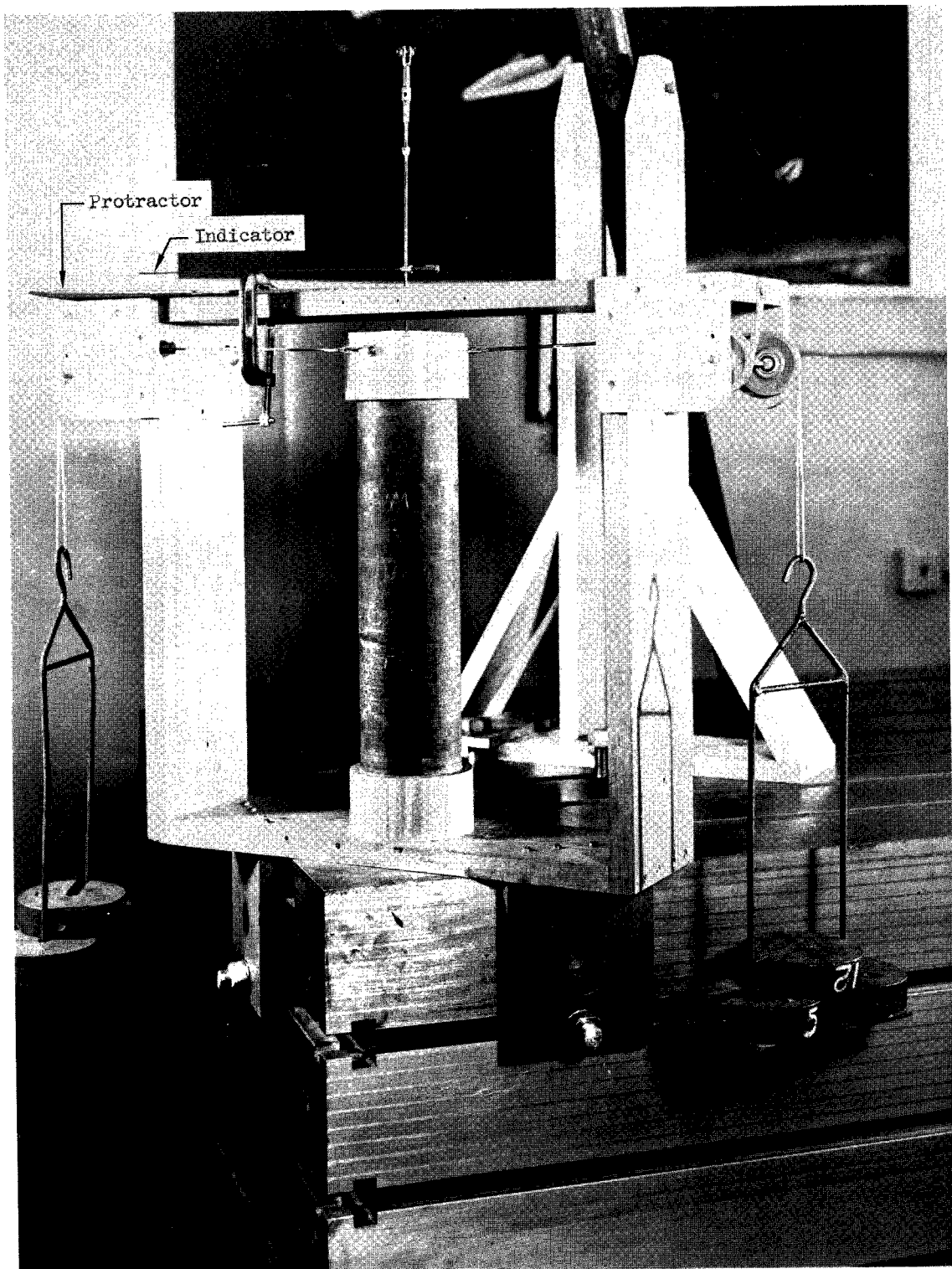
Figure 3.- Setup for torsion test on foam-filled cylinder.

L-61-3034.1

18
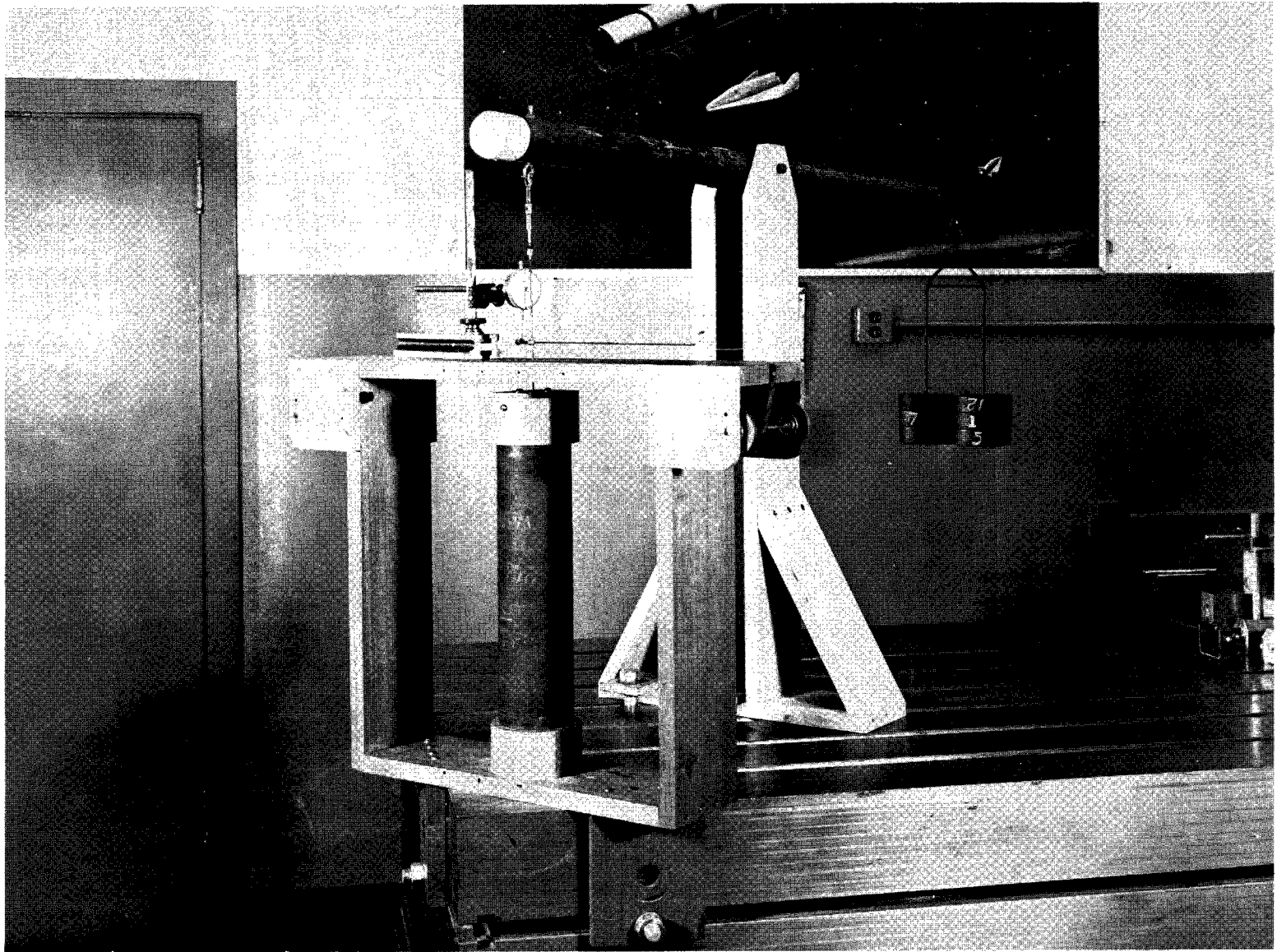
Figure 4.- Setup for tension test on foam-filled cylinder.

L-61-3035
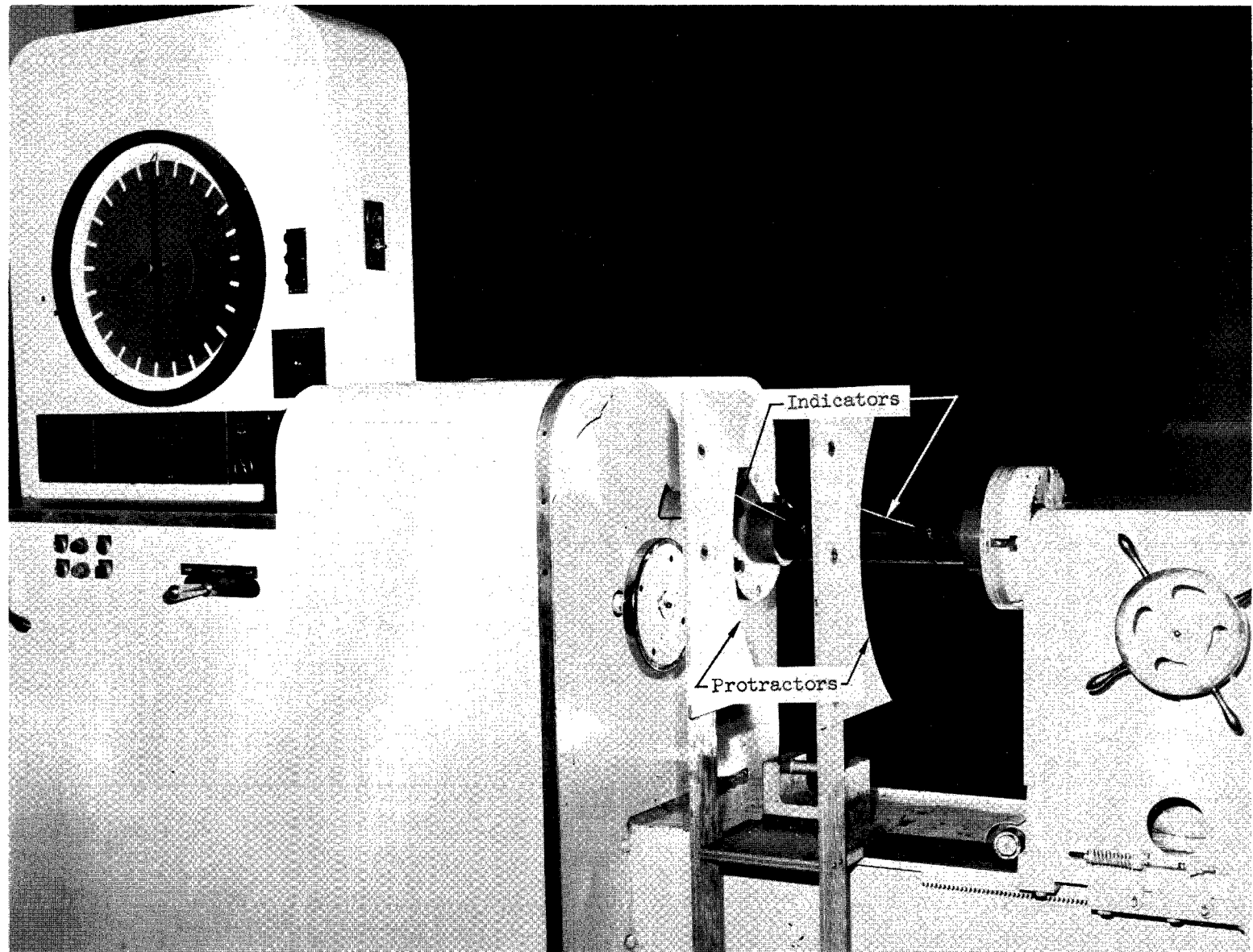
Figure 5.- Setup for torsion failure test on foam-filled cylinder.

L-63-1324.1
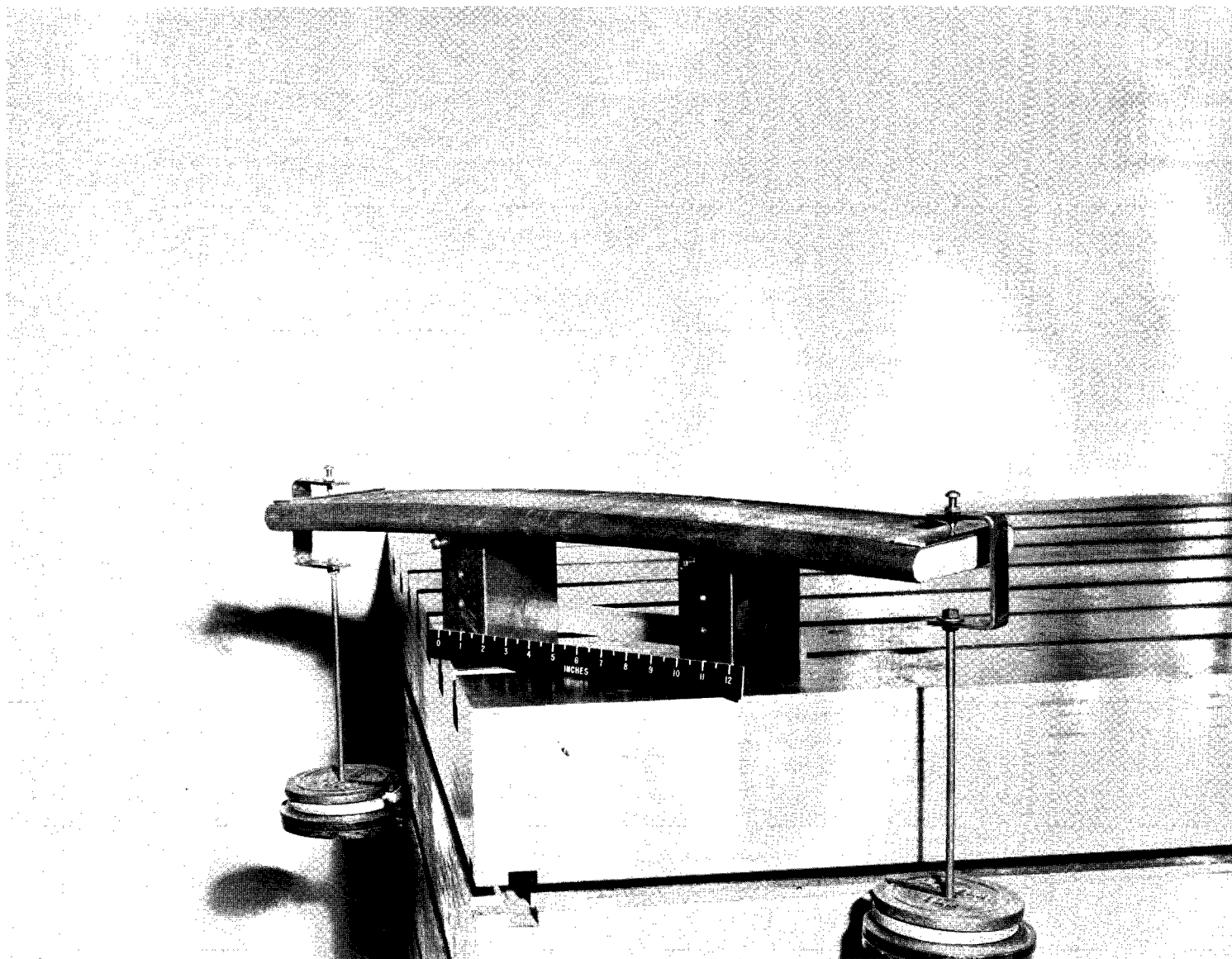
Figure 6.- Setup for bending test on foam-filled beam.

L-62-1697
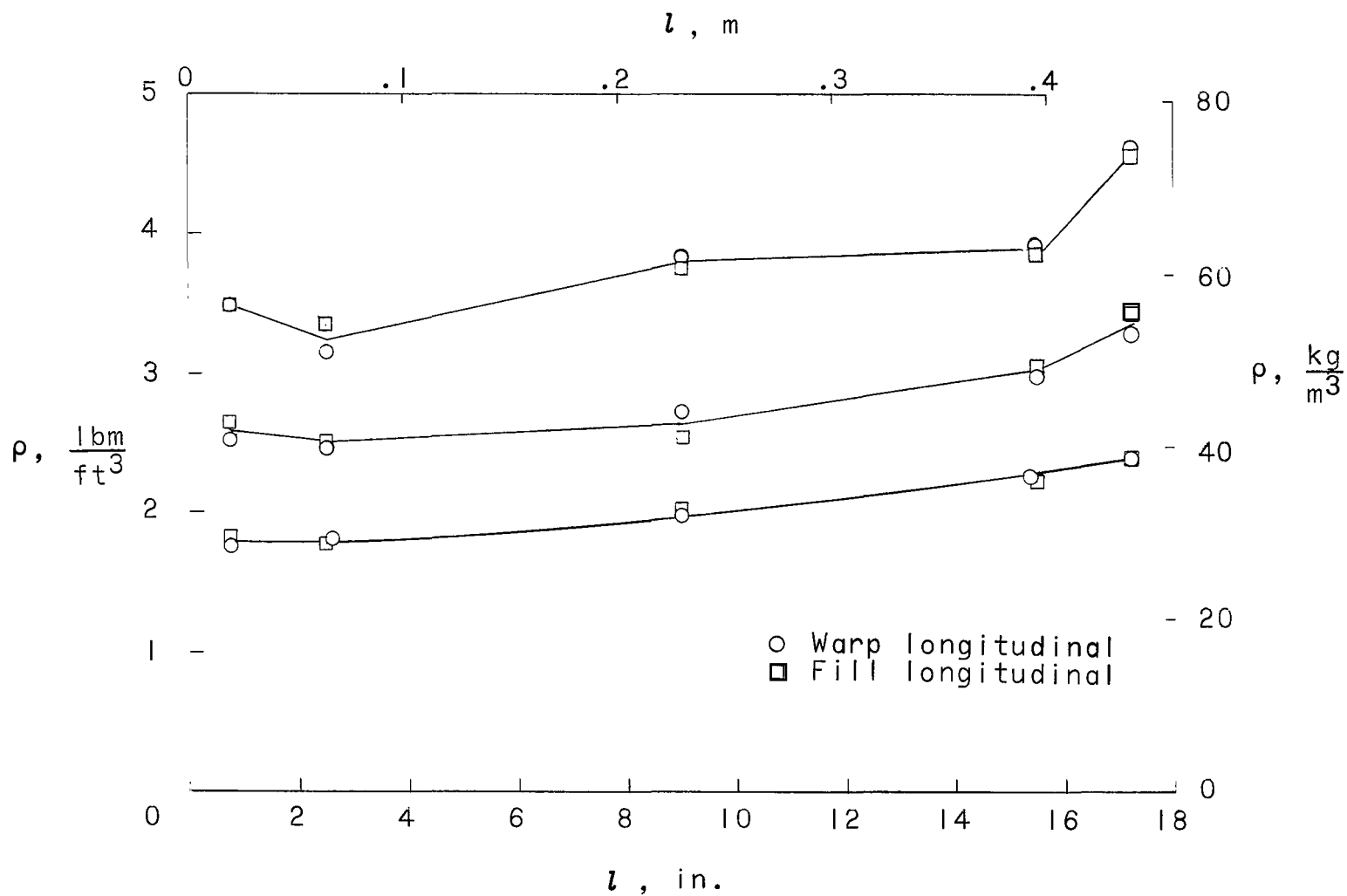
Figure 7.- Variation of foam density with cylinder length.
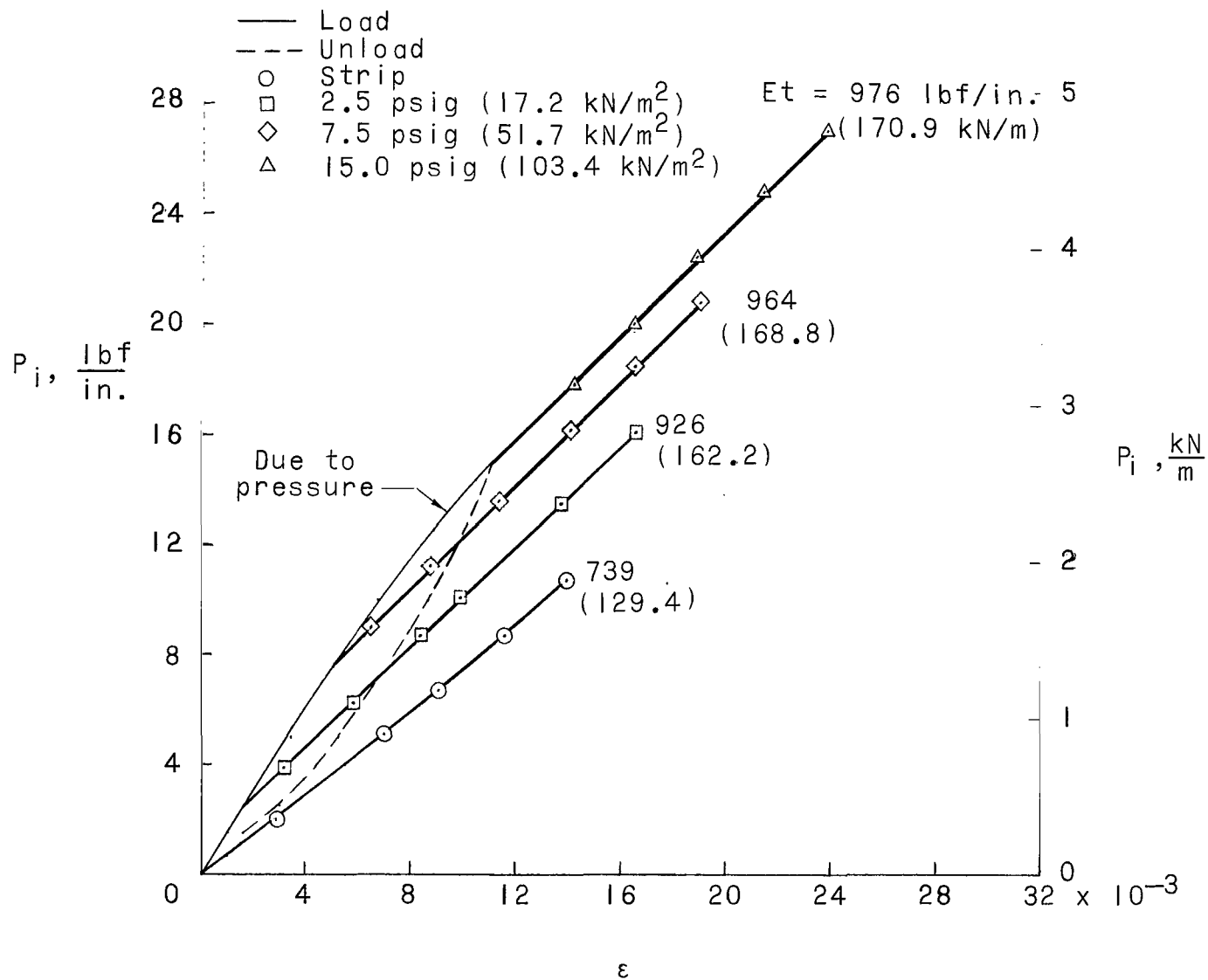
(a) Warp longitudinal.

Figure 8.- Typical stress-strain results for strip specimens and air-inflated cylinder specimens subjected to longitudinal tensile loads.
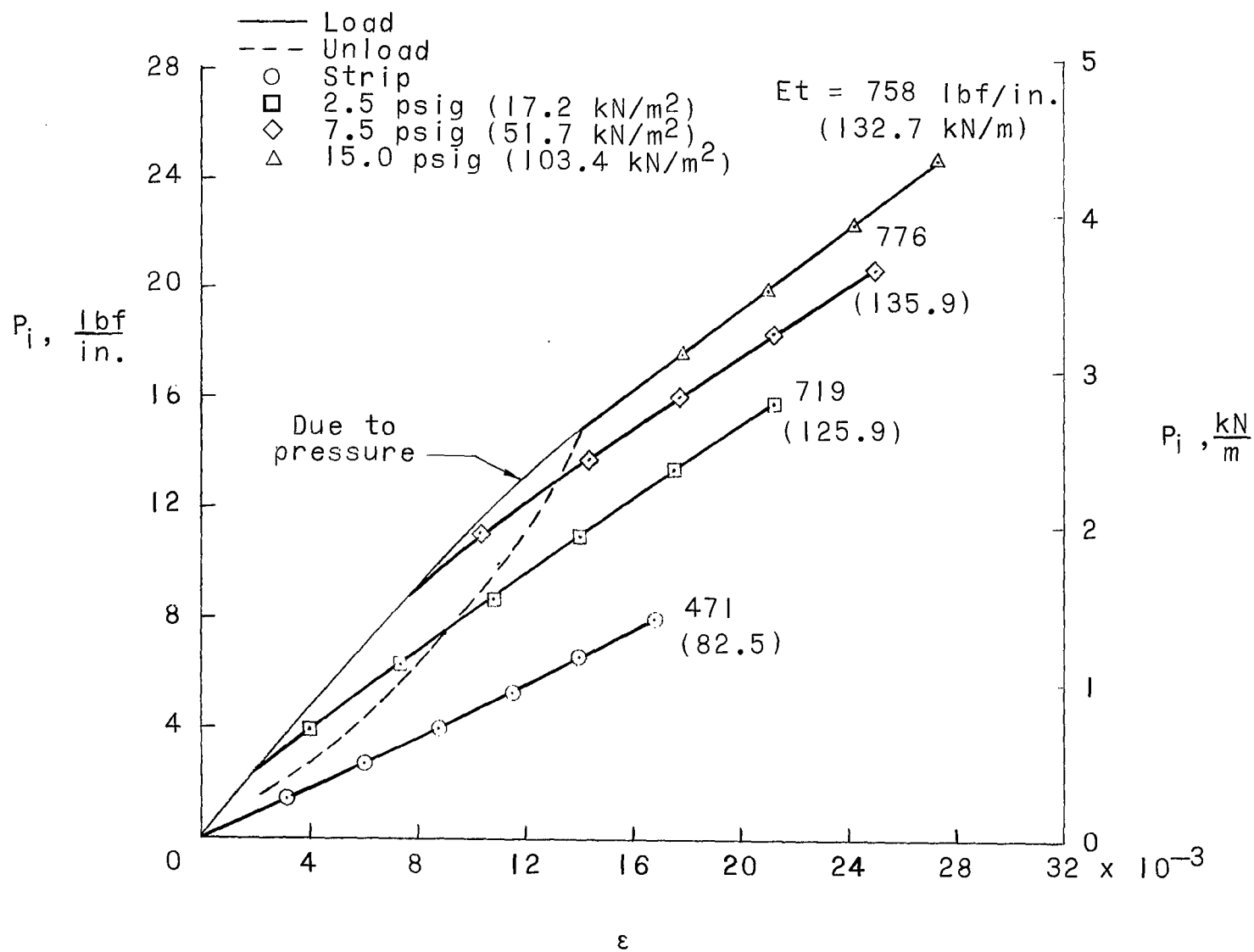
(b) Fill longitudinal.

Figure 8.- Concluded.
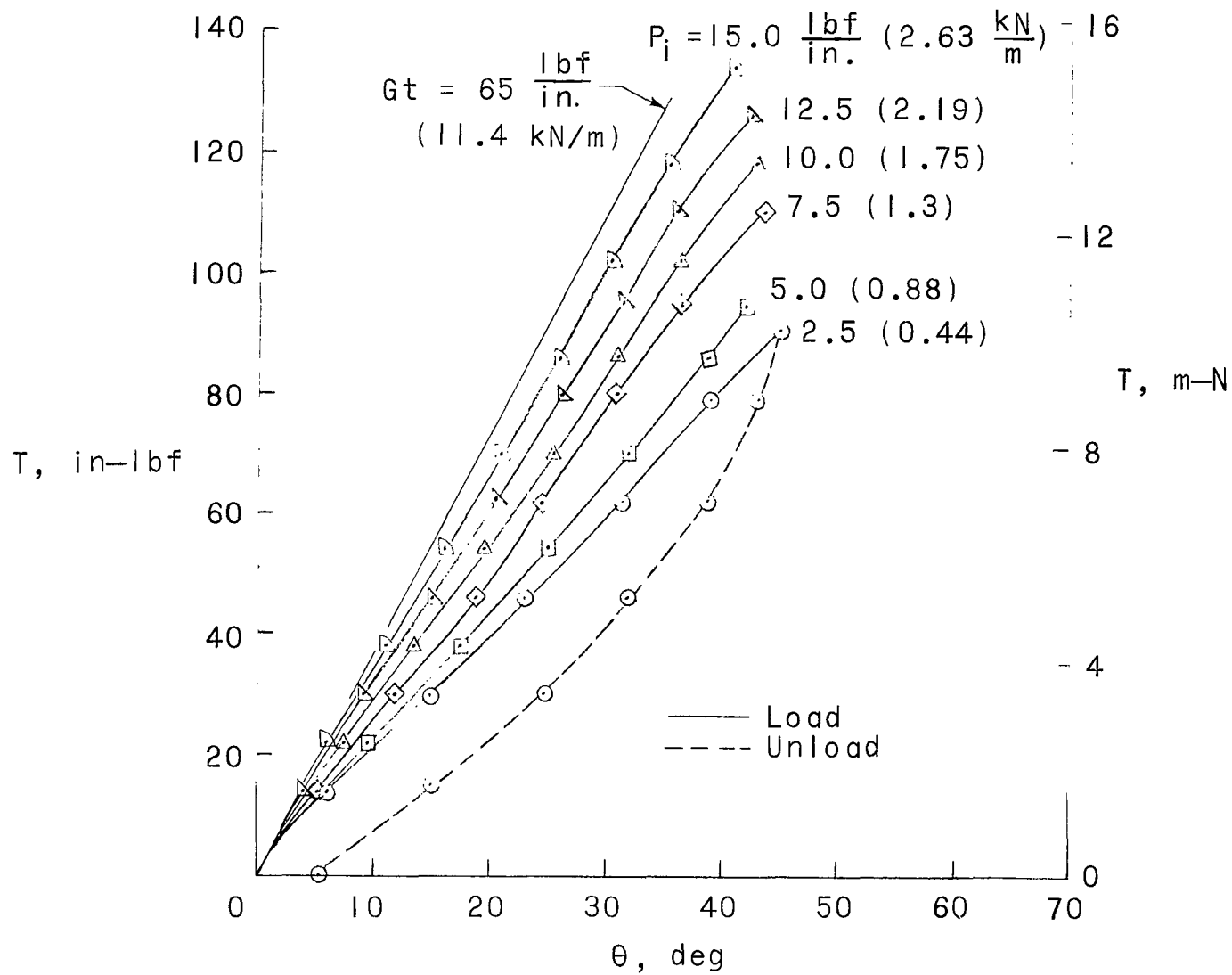
(a) Warp longitudinal.

Figure 9.- Torque plotted against twist for air-inflated cylinder specimens.
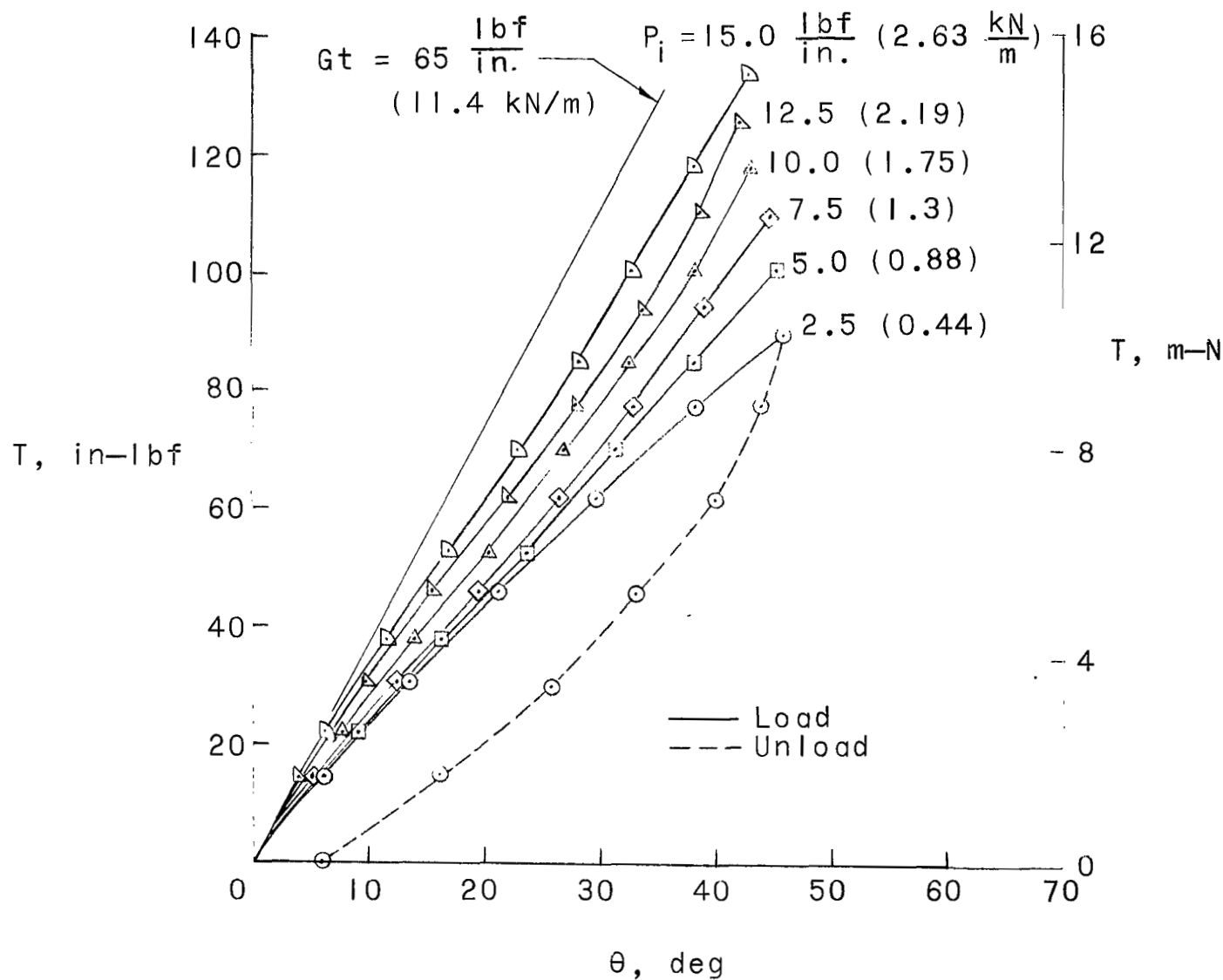
(b) Fill longitudinal.

Figure 9.- Concluded.
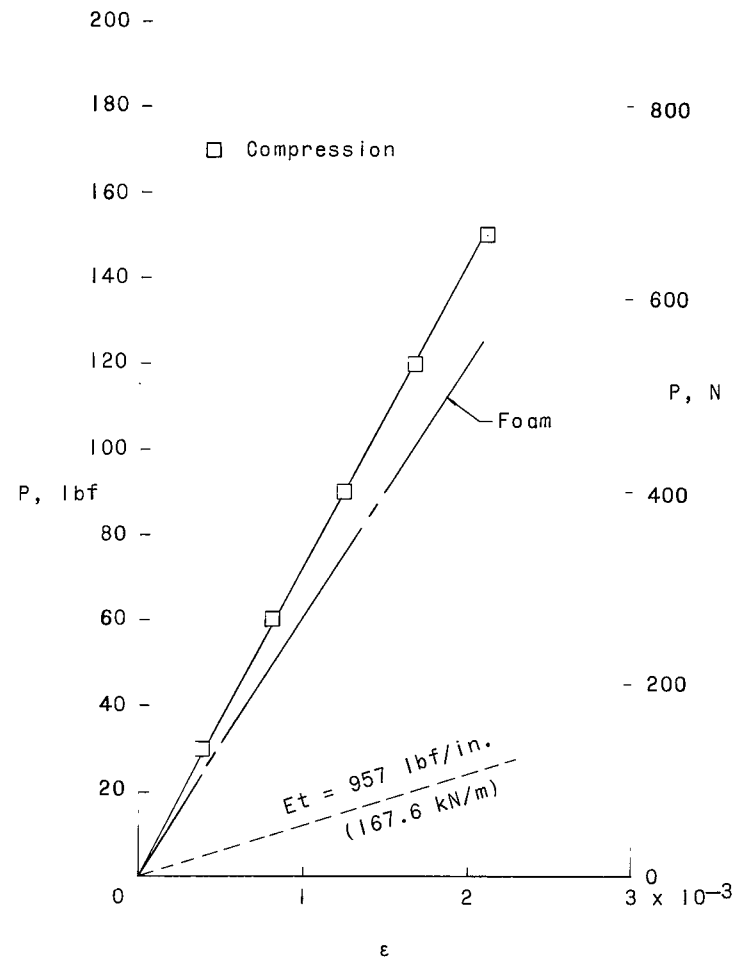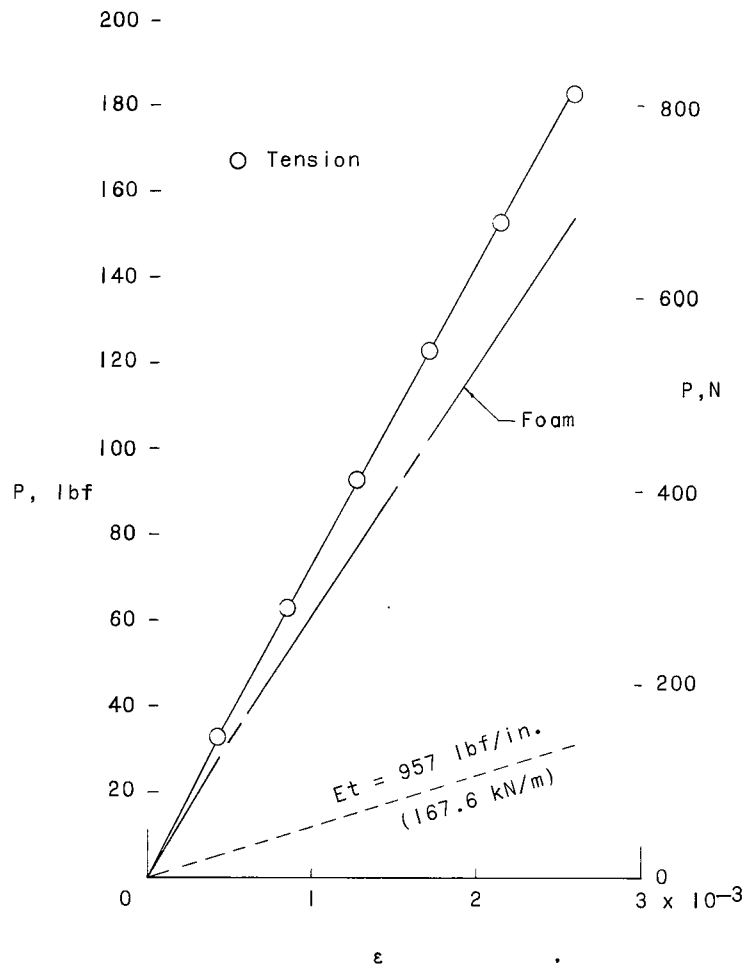
(a) Warp longitudinal.

Figure 10.- Typical load-strain results for foam-filled cylinder specimens subjected to longitudinal tensile and longitudinal compressive loads. ρ = 2.0 lbm/ft^3 (32.0 kg/m^3).
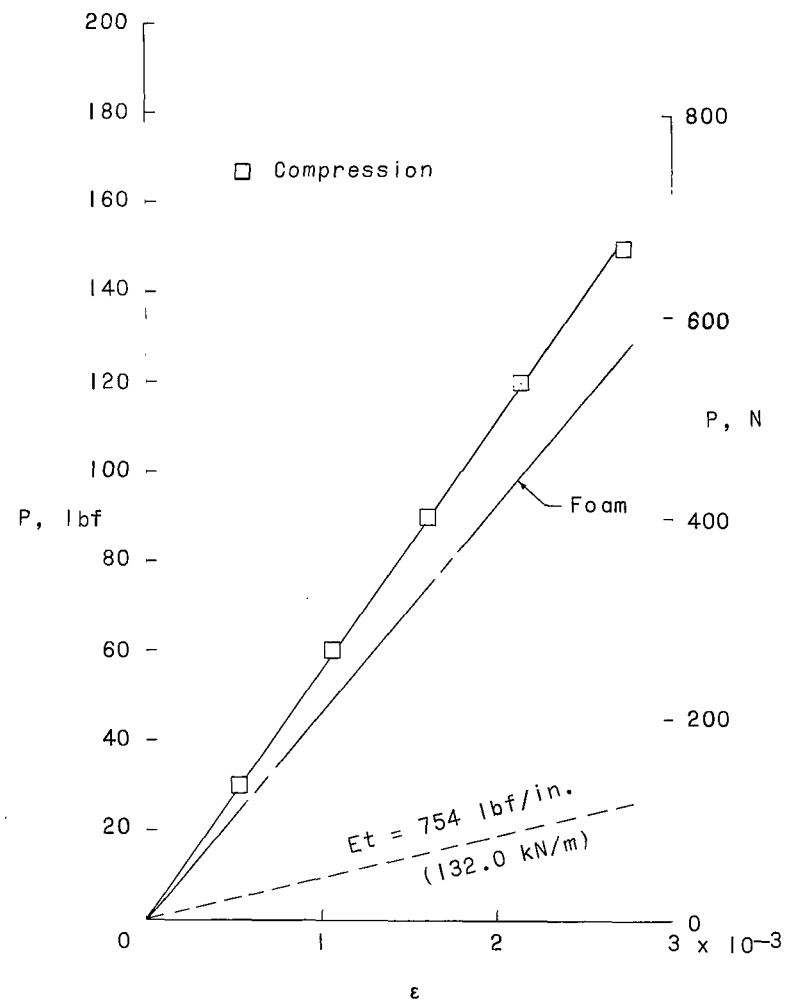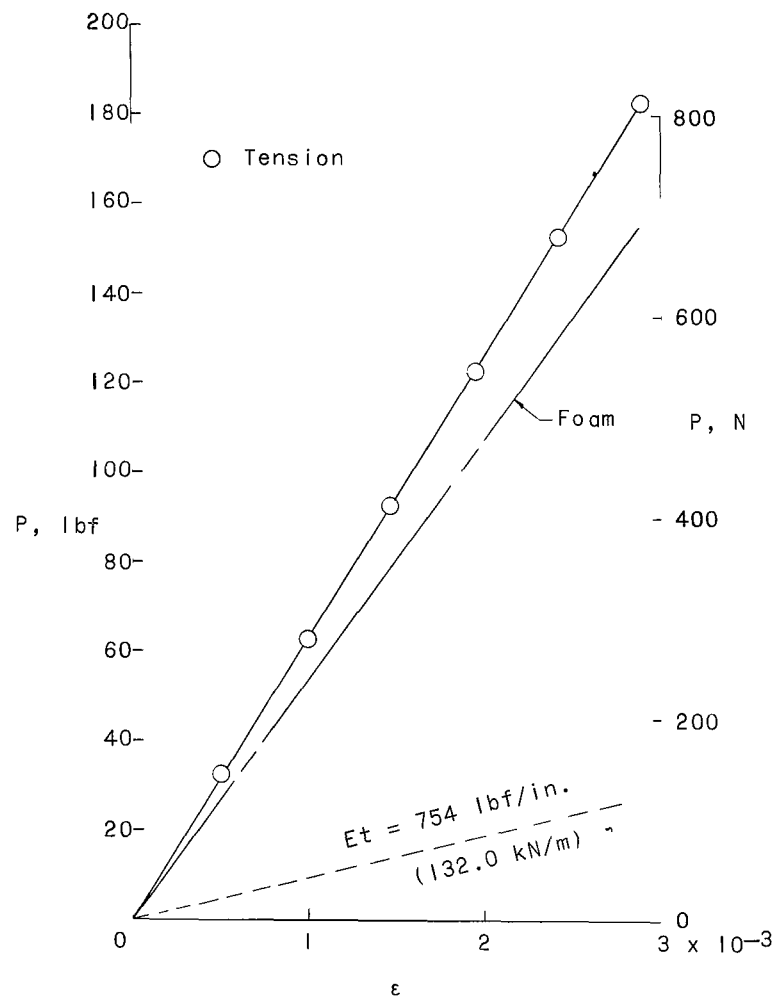
(b) Fill longitudinal.

Figure 10.- Concluded.
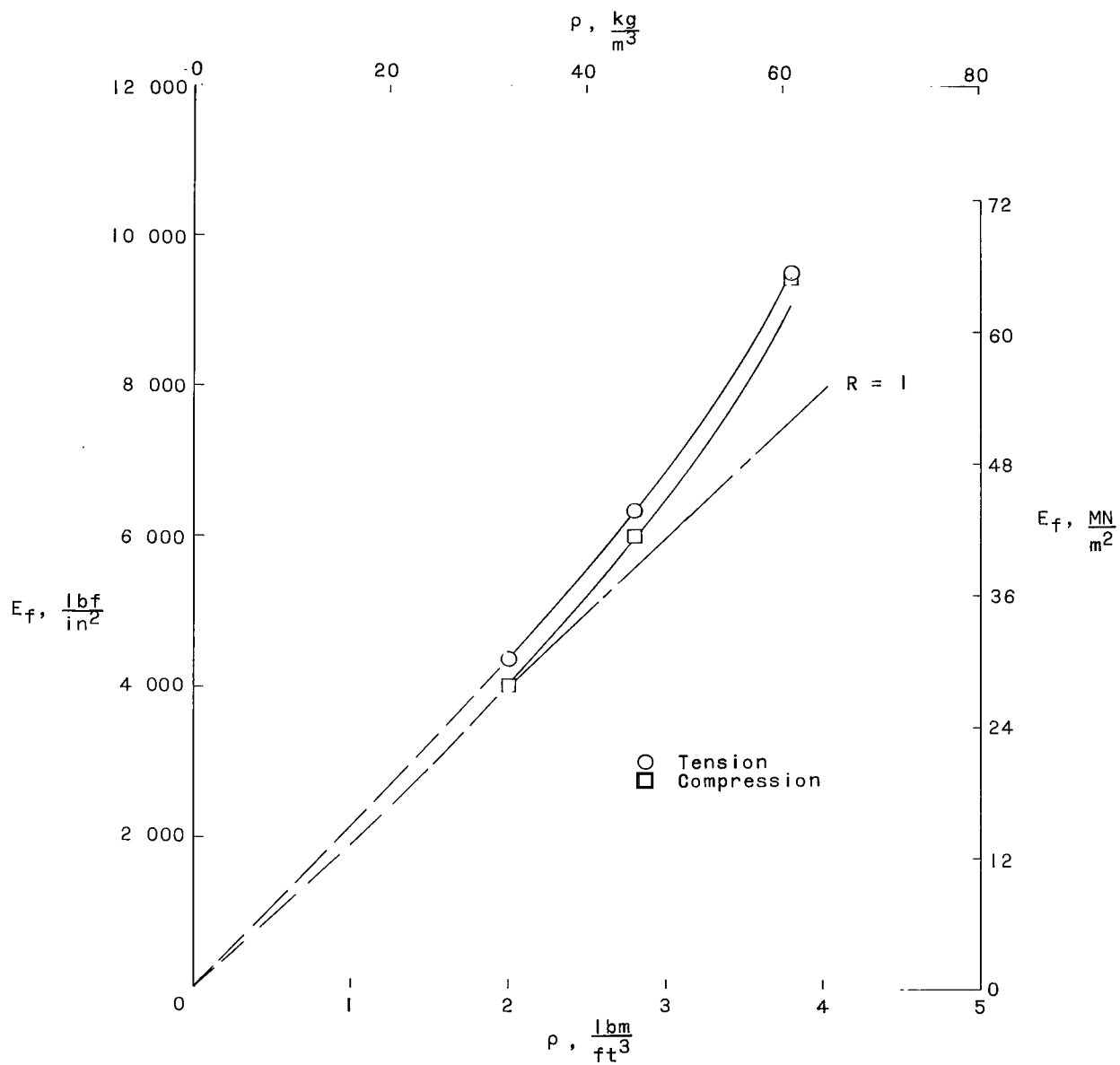
Figure 11.- Variation of Young's modulus with foam density for foam-filled cylinder specimens in tension or compression.
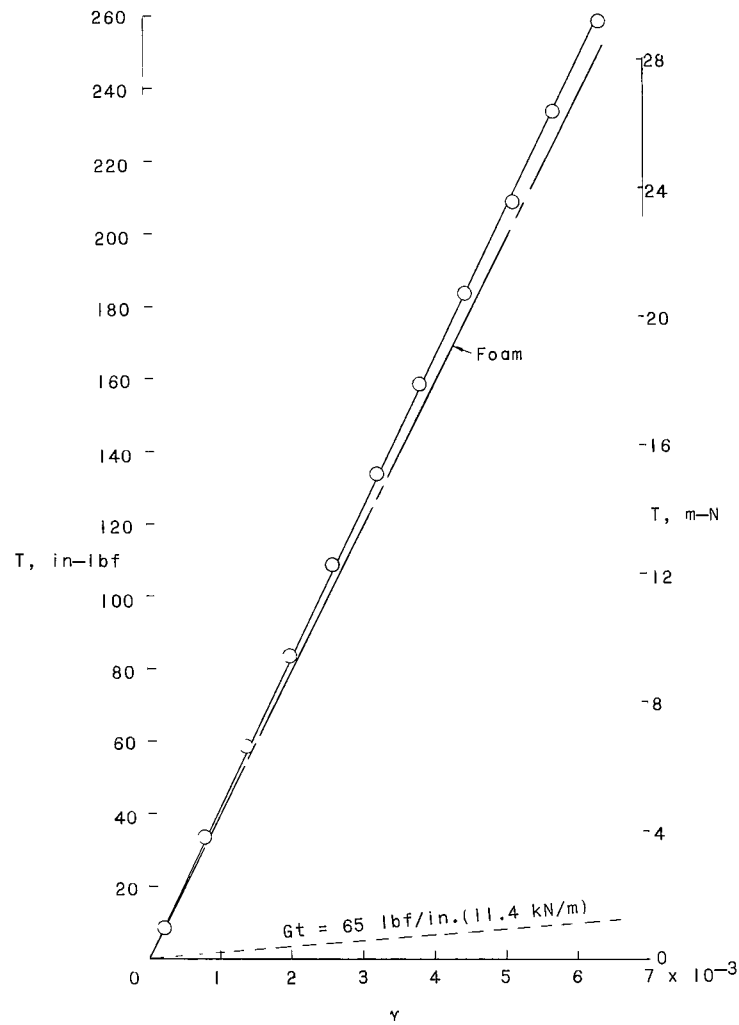
(a) Warp longitudinal.
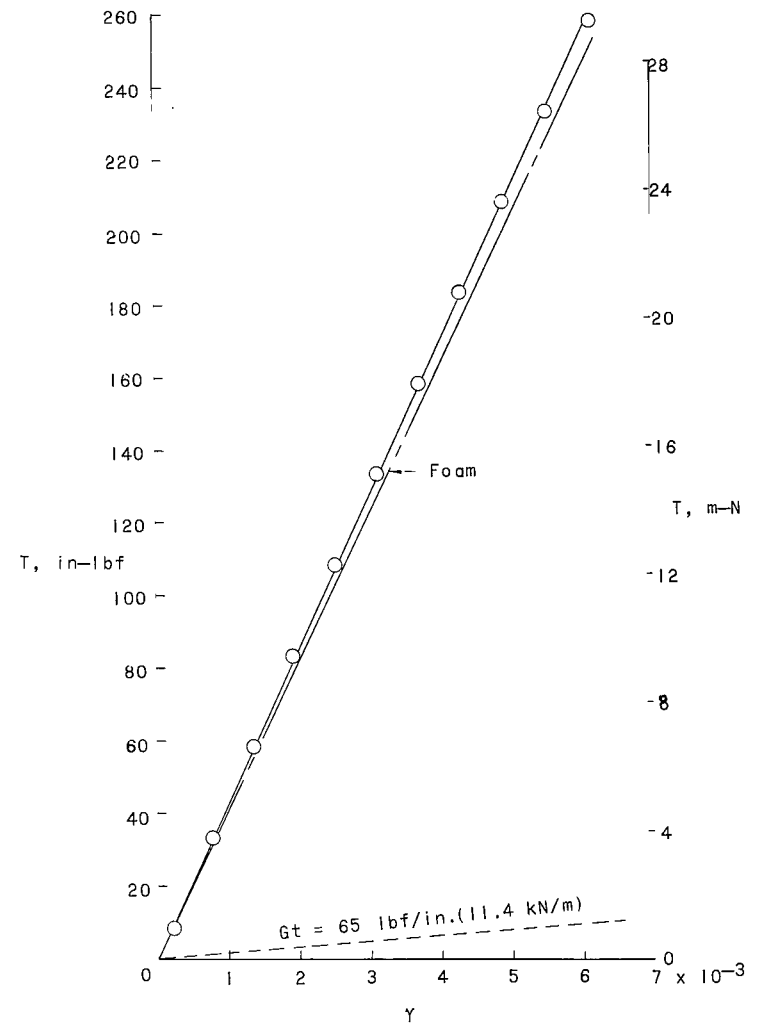
(b) Fill longitudinal.

Figure 12.- Typical torque—shear-strain results for foam-filled cylinder specimens subjected to small torsion loads. $\rho = 3.8$ lbm/ft^3 (60.9 kg/m^3).
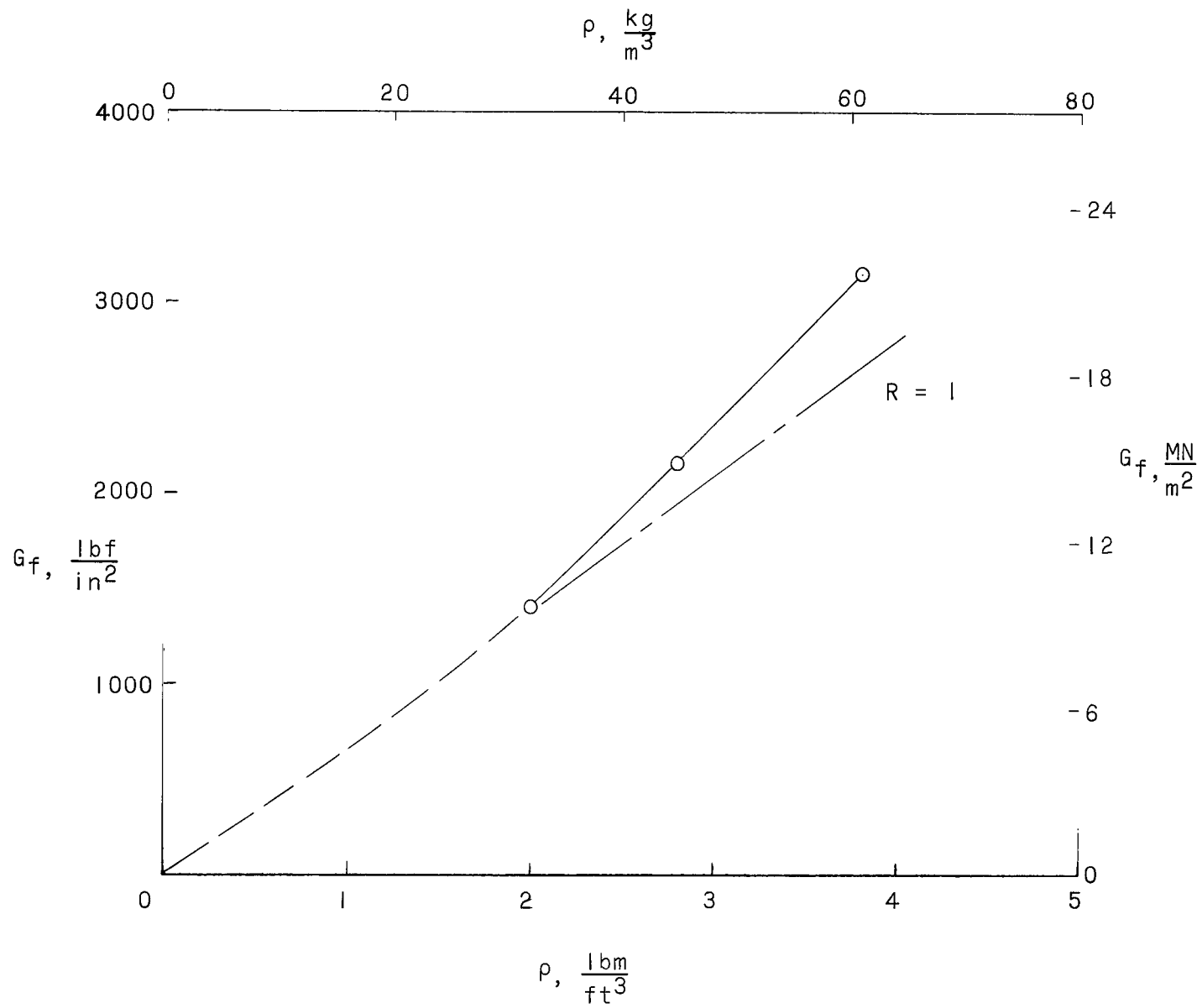
Figure 13.- Variation of shear modulus with foam density for foam-filled cylinder specimens.
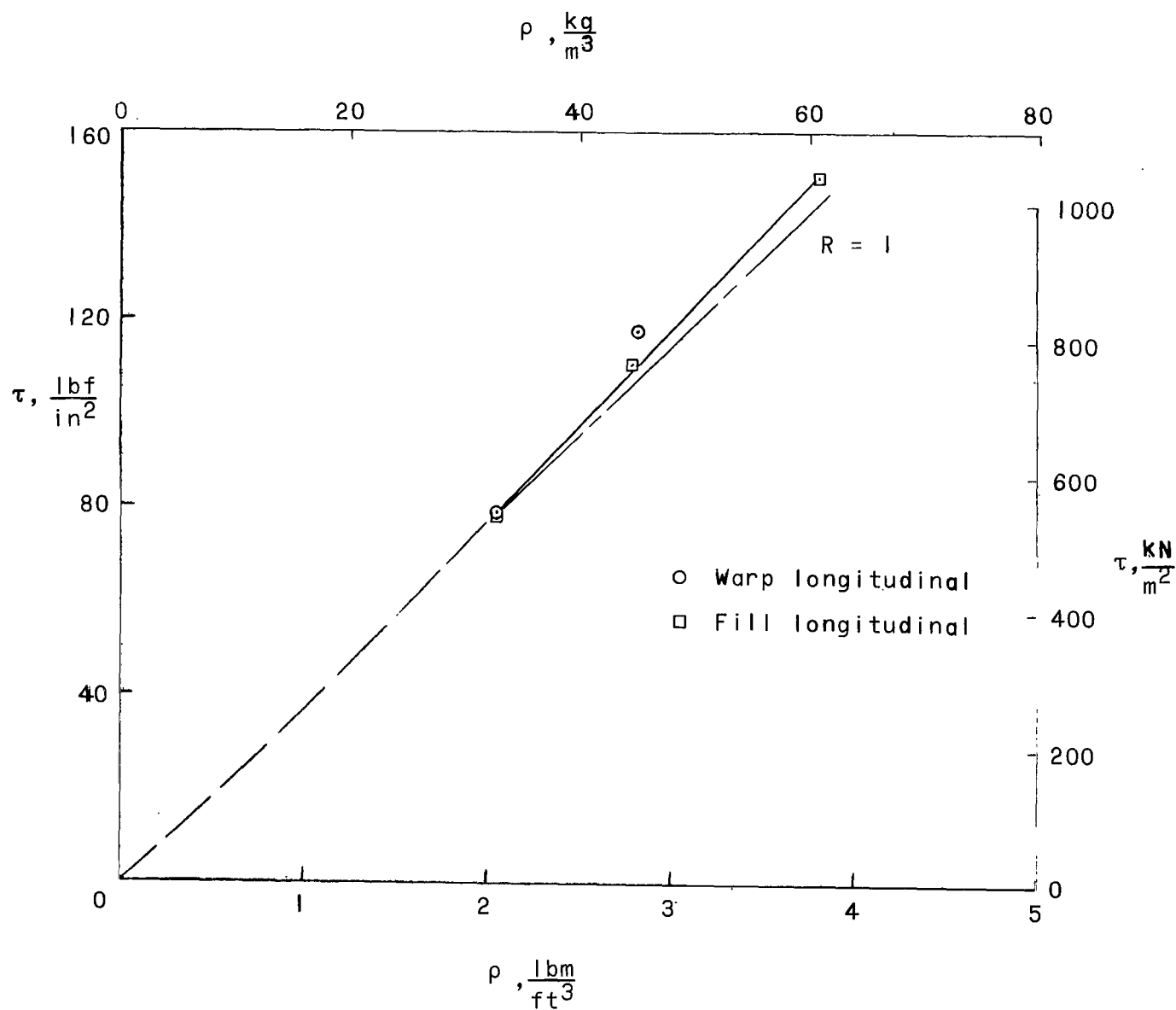
Figure 14.- Variation of torsion rupture modulus with foam density for foam-filled cylinder specimens.
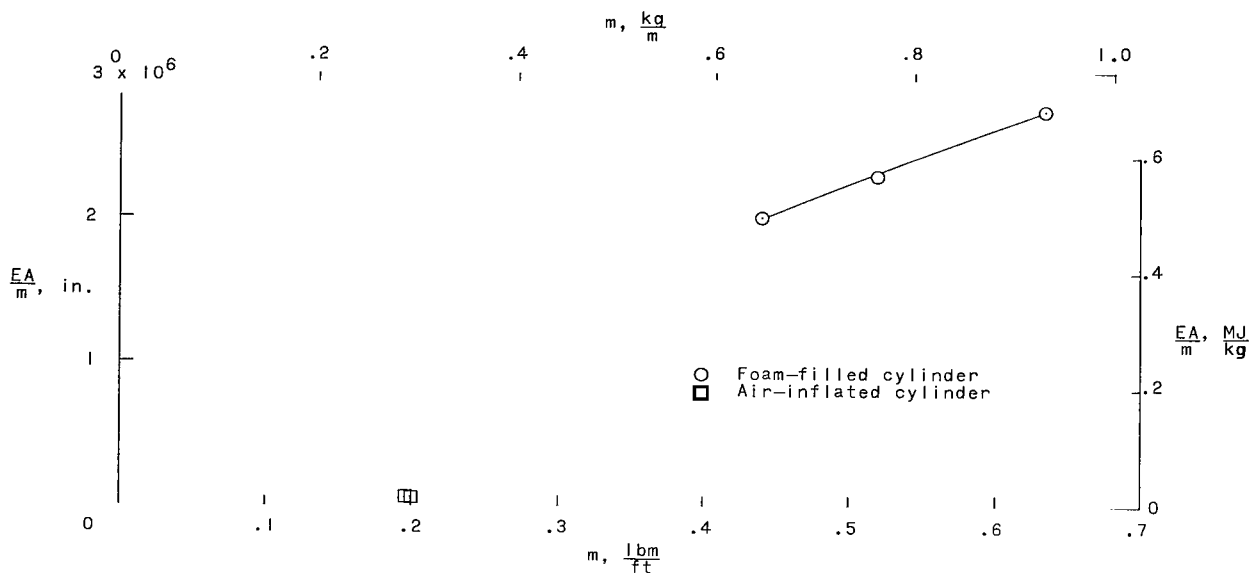
(a) Warp longitudinal.
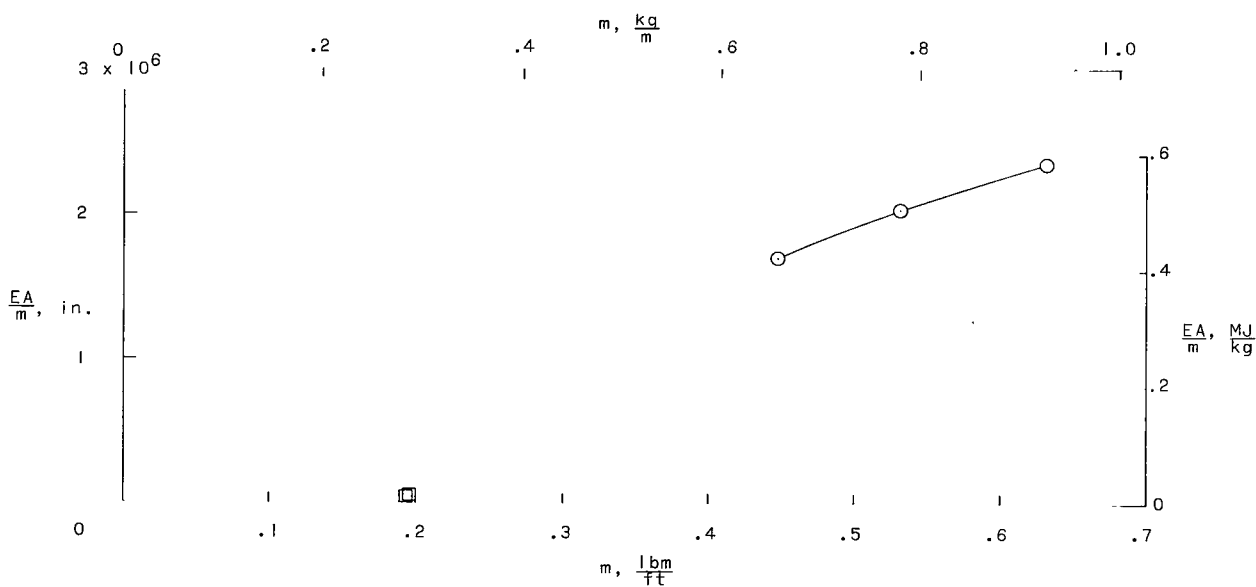
(b) Fill longitudinal.

Figure 15.- Specific-stiffness relations for cylinder specimens in tension.

.33
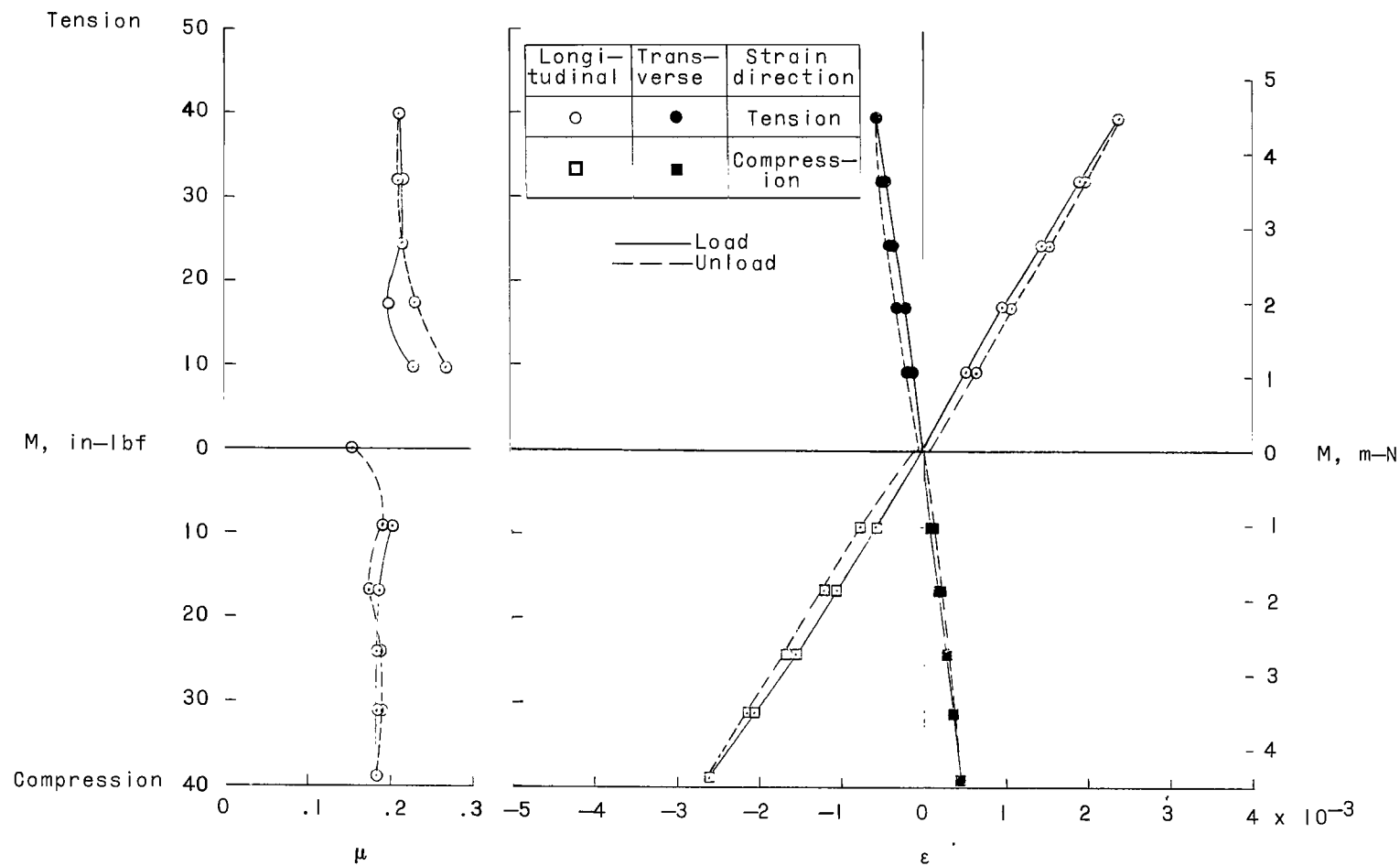
(a) Warp longitudinal. ρ = 4.5 lbm/ft^3 (72.1 kg/m^3).

Figure 16.- Typical bending-moment—strain characteristics and values of Poisson's ratio for foam-filled beam specimens in bending.
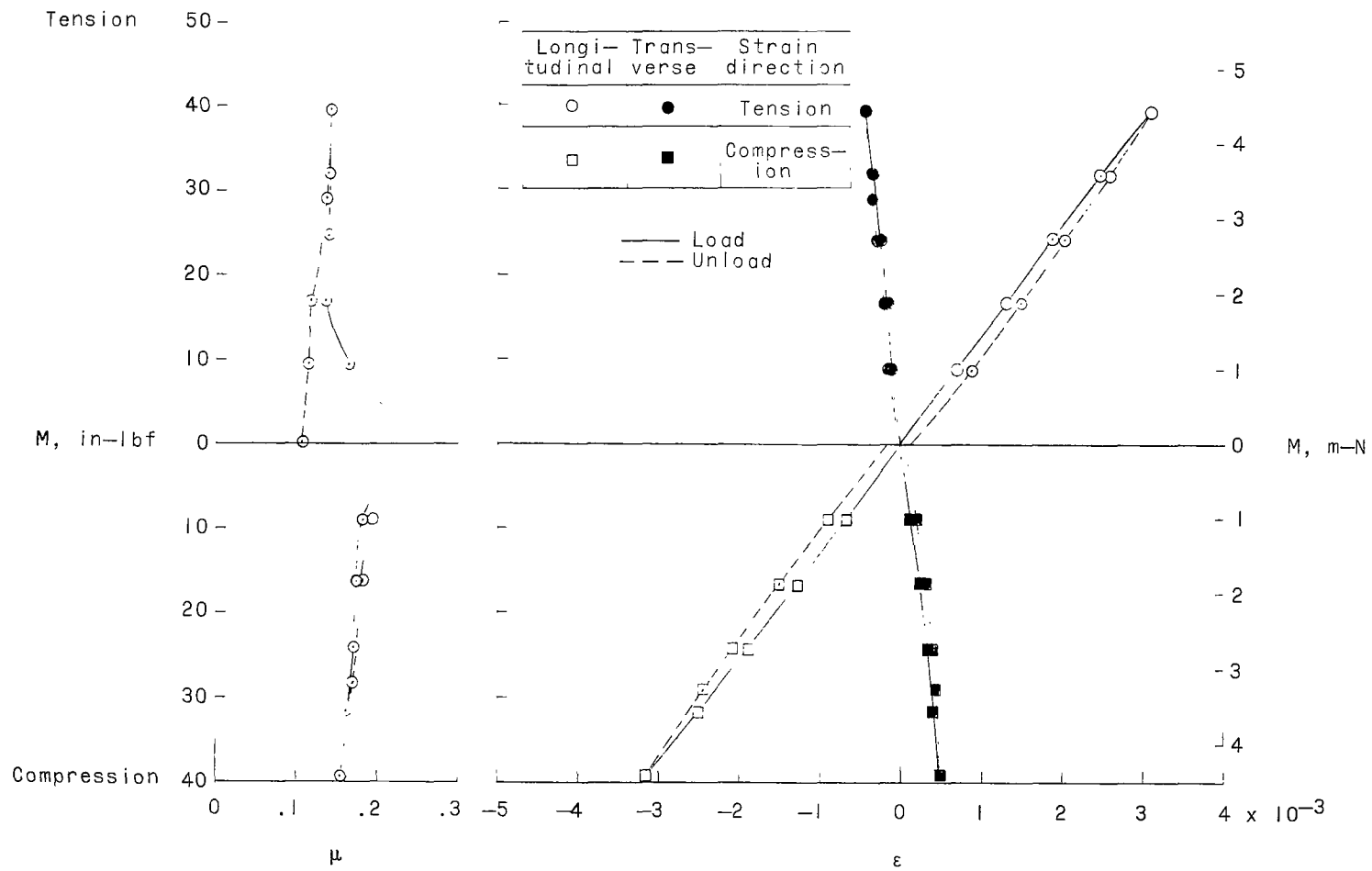
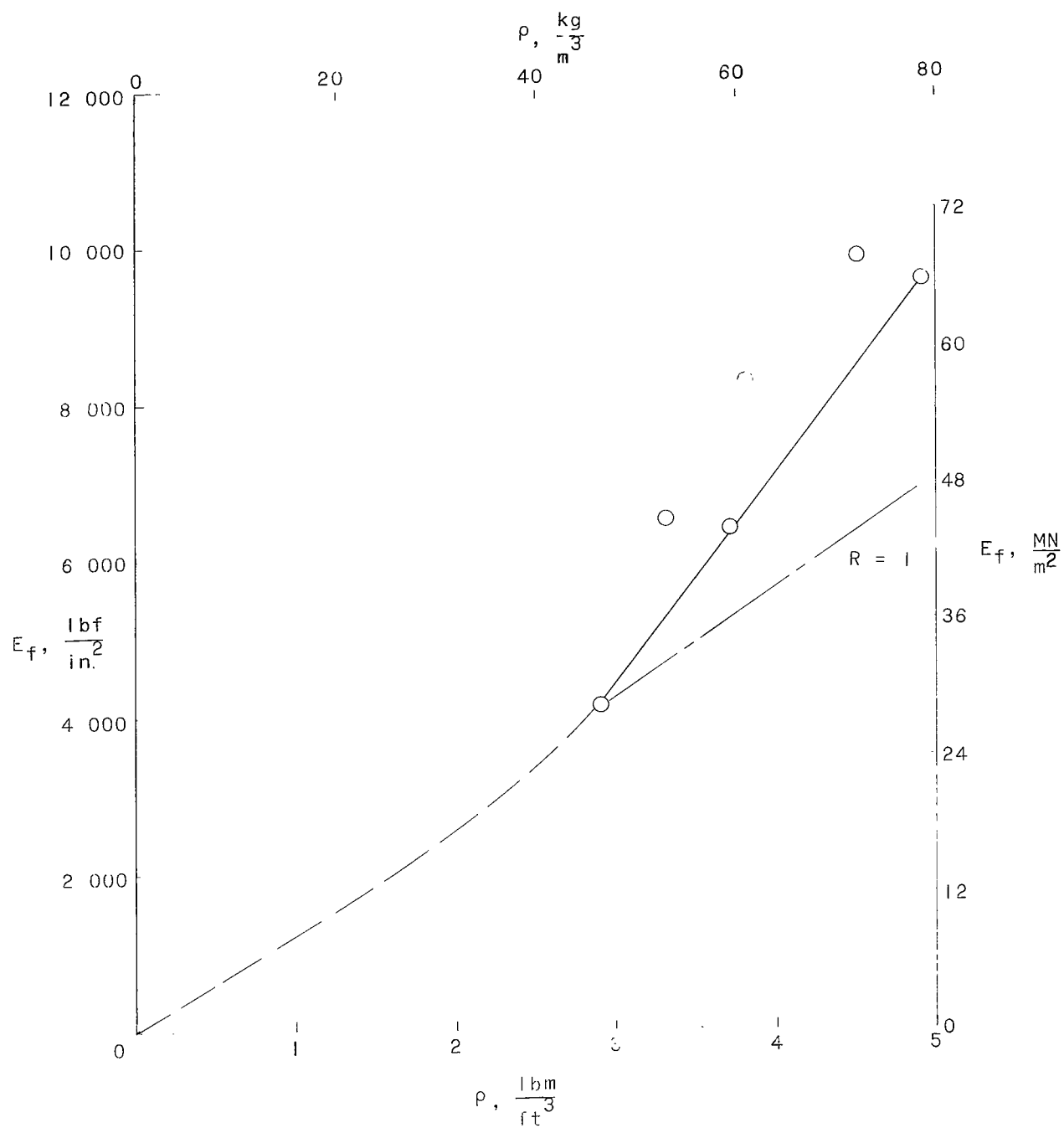(b) Fill longitudinal. $\rho = 4.9$ lbm/ft^3 (78.5 kg/m^3).

Figure 16.- Concluded.

Figure 17.- Variation of Young's modulus with foam density for foam-filled beams in bending.
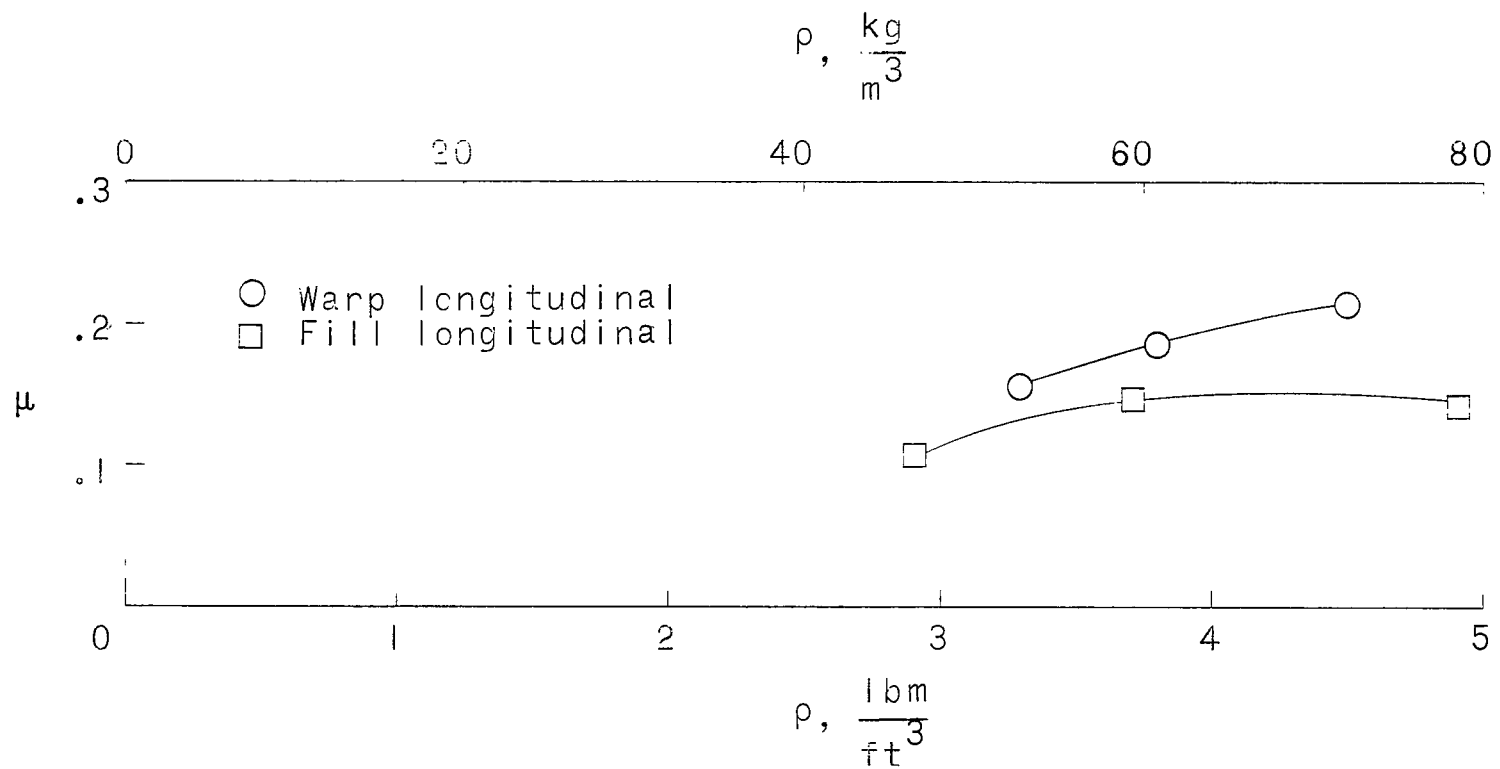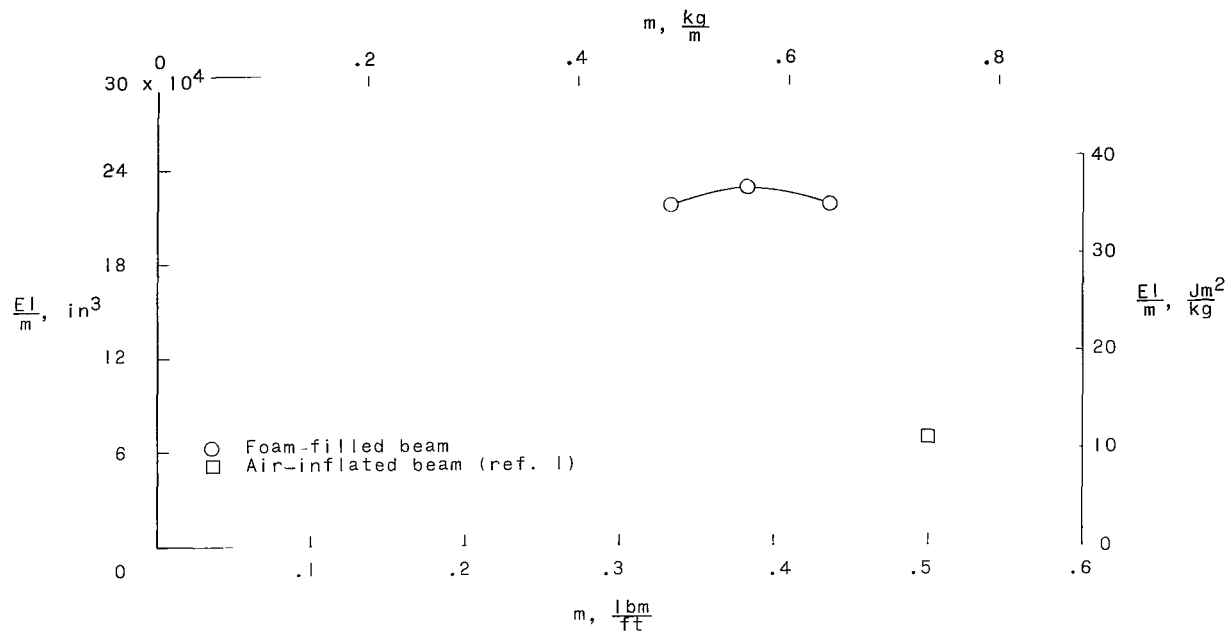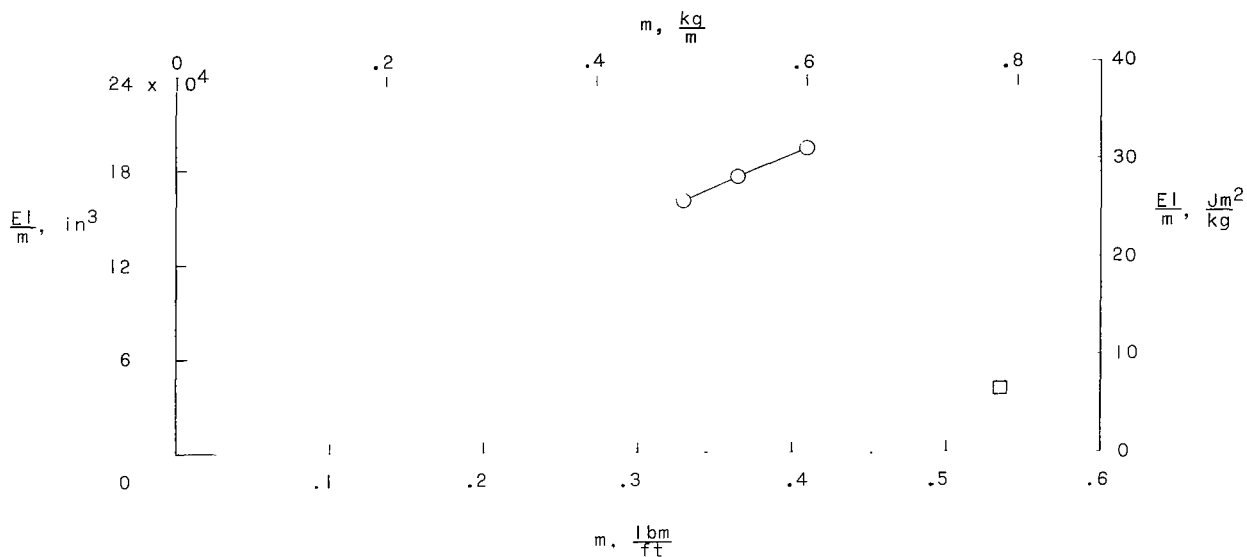
Figure 18.- Effect of foam density on average values of Poisson's ratio.

(a) Warp longitudinal.

(b) Fill longitudinal.

Figure 19.- Specific-stiffness relations for beam specimens.

"The aeronautical and space activities of the United States shall be conducted so as to contribute . . . to the expansion of human knowledge of phenomena in the atmosphere and space. The Administration shall provide for the widest practicable and appropriate dissemination of information concerning its activities and the results thereof."

—National Aeronautics and Space Act of 1958

NASA SCIENTIFIC AND TECHNICAL PUBLICATIONS

TECHNICAL REPORTS: Scientific and technical information considered important, complete, and a lasting contribution to existing knowledge.

TECHNICAL NOTES: Information less broad in scope but nevertheless of importance as a contribution to existing knowledge.

TECHNICAL MEMORANDUMS: Information receiving limited distribution because of preliminary data, security classification, or other reasons.

CONTRACTOR REPORTS: Technical information generated in connection with a NASA contract or grant and released under NASA auspices.

TECHNICAL TRANSLATIONS: Information published in a foreign language considered to merit NASA distribution in English.

TECHNICAL REPRINTS: Information derived from NASA activities and initially published in the form of journal articles.

SPECIAL PUBLICATIONS: Information derived from or of value to NASA activities but not necessarily reporting the results of individual NASA-programmed scientific efforts. Publications include conference proceedings, monographs, data compilations, handbooks, sourcebooks, and special bibliographies.

Details on the availability of these publications may be obtained from:

SCIENTIFIC AND TECHNICAL INFORMATION DIVISION

NATIONAL AERONAUTICS AND SPACE ADMINISTRATION

Washington, D.C. 20546